

# Noise induced unanimity and disorder in opinion formation

Agnieszka Kowalska-Styczeń<sup>1,\*</sup> and Krzysztof Malarz<sup>2,†</sup>

<sup>1</sup>*Silesian University of Technology, Faculty of Organisation and Management,  
ul. Roosevelta 26/28, 41-800 Zabrze, Poland*

<sup>2</sup>*AGH University of Science and Technology, Faculty of Physics and  
Applied Computer Science, ul. Mickiewicza 30, 30-059 Kraków, Poland*

(Dated: November 24, 2021)

We propose an opinion dynamics model based on Latané’s social impact theory. Actors in this model are heterogeneous and, in addition to opinions, are characterised by their varying levels of persuasion and support. The model is tested for two and three initial opinions randomly distributed among actors. We examine how the noise (randomness of behaviour) and the flow of information among actors affect the formation and spread of opinions. Our main research involves the process of opinion formation and finding phases of the system in terms of parameters describing noise and flow of the information for two and three opinions available in the system. The results show that opinion formation and spread are influenced by both (i) flow of information among actors (effective range of interactions among actors) and (ii) noise (randomness in adopting opinions). The noise not only leads to opinions disorder but also it promotes consensus under certain conditions.

Keywords: Complex systems; Opinion dynamics; Social modelling; Nowak–Szamrej–Latané model; Long range interactions; Agent based simulations

arXiv:2002.05451v2 [physics.soc-ph] 3 May 2020

---

\*  0000-0002-7404-9638; [Agnieszka.Kowalska-Styczen@polsl.pl](mailto:Agnieszka.Kowalska-Styczen@polsl.pl)

†  0000-0001-9980-0363; [malarz@agh.edu.pl](mailto:malarz@agh.edu.pl)

## I. INTRODUCTION

Understanding how opinions are formed and spread in society is very important in studying consumer behaviour, organisational behaviour, predicting election results, and many others. As pointed out by Acemoglu and Ozdaglar [1], we acquire our opinions and beliefs in the process of social learning, during which people get information and update their opinions as a result of their own experience, as well as observation of other people’s activities and from their experience. This process takes place in a social network consisting of friends, co-workers, family members and a certain group of leaders that we listen to and respect [1, 2]. Units update and create their views by communicating with other people who belong to their social network. It is communication that connects people and creates relationships [3].

It should be noted that people often copy the choices of others [4, 5]. This applies, for example, to the choice of names for children [6, 7], a popular book, dishes ordered in a restaurant (instead of studying the menu, we look at what the others have ordered), and even ideological beliefs [5]. This copying of opinions and behaviours often takes place in a network of informal contacts and it is based on social relations between people [8] and plays an important role in forming opinions. In addition, we are often dealing with unpredictability or indifference in opinion-forming or decision-making (despite the positive attitude towards the proposed actions). This applies, among others, to electricity tariffs, eco-innovations or pro-environmental attitudes [9–11], as well as voting behaviour [12], in which human rationality is bounded. One of the most active discussions in psychology of the opinion dynamics is also about the irrational processing of information [13], therefore, this aspect should be taken into account in studying opinion formation. Furthermore, individuals belong to many groups, or have many interactions outside the main group (a group of closest neighbours). Such a connection with people from other groups (neighbourhoods) increases the information advantage [14], and can be interesting in disseminating information.

We therefore propose a model of forming an opinion based on the social impact theory formulated by Latané [15], in which we take into account the randomness of the actors’ behaviour by introducing a noise (social temperature), as well as interactions with agents; not only close neighbours, but in the whole network by  $\alpha$  parameter (scale the distance function). Our agents are heterogeneous through a different level of persuasion intensity and support intensity, as well as the possibility of having different opinions.

Recently, the multi-choice opinion dynamics model [16, 17] based on Latané theory [15, 18–21] was proposed. In this model, it is possible to test the diffusion of opinions in case there are more than two opinions available in the system. The earlier attempts to modelling multiple-choice of opinions include among others multi-state and discrete-state opinions models [22–32] or discrete vector-like variables [33–36]. The rest of huge literature (see papers by Sirbu *et al.* [37], Castellano *et al.* [38], Stauffer [39], Anderson *et al.* [40], and Galam [41] for reviews) is devoted to the systems with binary opinions (see for example Refs. 42–45) or the continuous space of opinions (see for example Refs. 13, 46–62).

There are also many examples showing that randomness is useful and beneficial. Random noise facilitates the dynamics and reduces relaxation times in the models of social influence [63]. In addition, noise plays a beneficial role in developing cooperation [64], in the application of social and financial strategies [65] and in addressing the coordination problem of human groups [66].

In this paper we study how opinions are formed and how they spread in the community. Agent based model with lattice fully populated by actors has been adopted, where each of the network nodes refers to one person. We take into account the flow of information in the community (effective range of actors interactions) and noise (randomness of human behaviour). We show with computer simulation, that small level of noise induces unanimity of opinion. Unfortunately, this beneficial noise role was overlooked in Ref. 16 due to unreasonable extrapolation of results for middle noise level towards noiseless system.

## II. MODEL

To study the diffusion of opinions, the theory of social influence introduced by Latané [15] in the dynamic manner proposed by Nowak *et al.* [21]—as implemented by Bańcerowski and Malarz [16]—has been used.

Social influence is a process that results in a change in the behaviour, opinion or feelings of a human being as a result of what other people do, think or feel. The essence of social influence is of course not only exerting social influence, but also succumbing to it, which will be taken into account in the used model by means of appropriate parameters (intensity of persuasion and intensity of support). The Latané [15] theory rely on three experimentally proven [18–20] assumptions:

**social force principle:** it says that social impact  $I$  (details are given in description of Eq. (2)) on  $i$ -th actors is a function of the product of strength  $S$ , immediacy  $J$ , and the number of sources  $N$ ; The strength of influence is

the intensity, power or importance of the source of influence. This concept may reflect socio-economical status of the one that affects our opinion, his/her age, prestige or position in the society. The immediacy determines the relationship between the source and the goal of influence. This may mean closeness in the social relationship, lack of communication barriers and ease of communication among actors;

**psycho-social law:** it states that each next actor  $j$  sharing the same opinion as actor  $i$  exerts the lower impact on the  $i$ -th actor;

**division of impact theory:** it is based on the bystander effect and is observed as the errors of reacting to crisis events, along with an increase in the number of witnesses to this event.

Based on these assumptions Nowak *et al.* [21] proposed computerised model of opinion dynamics based on Latané [18–20] social impact theory (see Ref. 67 for review).

Every agent  $i$  is characterised by the following parameters:

**opinion**  $\xi_i$ : the current opinion supported by agent  $i$ ,

**intensity of support**  $s_i$ : the strength of the agent  $i$  influence on other agents, which determines the ability of this agent to convince other agents not to change their opinion if this opinion is identical to his/her opinion ( $0 \leq s_i \leq 1$ ),

**intensity of persuasion**  $p_i$ : the strength of agent  $i$  influence on agents, which determines the ability of this agent to convince other agents to accept his/her opinions ( $0 \leq p_i \leq 1$ ).

Each agent is influenced by all other agents on the network. The strength of this influence decreases as the distance between agents increases. In the presented model a cellular automaton was used, which consists of a square grid of  $L^2$  cells, where exactly one agent is assigned to each cell. The distance  $d_{ij}$  between agents  $i$  and  $j$  is calculated as the Euclidean distance between cells.

To take into account the varied flow of information in the community, we use the  $\alpha$  parameter, which was adapted to scale the distance function. Parameter  $\alpha$  adjusts the influence of close and distant neighbours in the community. Small  $\alpha$  values mean good communication between agents and good access to information, because it allows for an exchange of information with a large number of agents in the network. The larger values of  $\alpha$ , weaker the communication among the groups of agents, weaker effective exchange of information and weaker access to information, because the exchange of information takes place only in the closest neighbourhood of actors, although we still keep long-range interactions among actors.

Here we are on a position to recapitulate the formal model composition as proposed in Ref. 16.

## A. Formal model description

Actors occupy the nodes of the square lattice with linear size  $L$ . Every actor  $1 \leq i \leq L^2$  is characterised by his/her discrete opinion  $\xi_i \in \{\Xi_1, \Xi_2, \dots, \Xi_K\}$ , where  $K$  is the number of opinions available in the system. Additionally, we assign random real value  $p_i \in [0, 1]$  and  $s_i \in [0, 1]$  describing actor's persuasiveness and his/her supportiveness, respectively.

The system evolution depends on the social temperature  $T$ . If  $T = 0$ , then a lack of noise is assumed, and the actor  $i$  adopts an opinion  $\Xi_k$  that has the most impact on it:

$$\xi_i(t+1) = \Xi_k \iff I_{i,k}(t) = \max(I_{i,1}(t), I_{i,2}(t), \dots, I_{i,K}(t)), \quad (1)$$

where  $k$  is the label of this opinion which believers exert the largest social impact on  $i$ -th actor and  $I_{i,k}$  are the social influence on actor  $i$  exerted by actors sharing opinion  $\Xi_k$ .

The social impact on actor  $i$  from actors  $j$  sharing opinion of actor  $i$  ( $\xi_j = \xi_i$ ) is calculated as

$$I_{i,k}(t) = 4\mathcal{J}_s \left( \sum_{j=1}^N \frac{q(s_j)}{g(d_{i,j})} \delta(\Xi_k, \xi_j(t)) \delta(\xi_j(t), \xi_i(t)) \right) \quad (2a)$$

while  $K - 1$  social impacts on actor  $i$  from all other actors having  $K - 1$  different opinions ( $\xi_j \neq \xi_i$ ) is given as

$$I_{i,k}(t) = 4\mathcal{J}_p \left( \sum_{j=1}^N \frac{q(p_j)}{g(d_{i,j})} \delta(\Xi_k, \xi_j(t)) [1 - \delta(\xi_j(t), \xi_i(t))] \right), \quad (2b)$$

where  $1 \leq k \leq K$  enumerates the opinions and Kronecker's delta  $\delta(x, y) = 1$  if  $x = y$  and zero otherwise [16].

As in Ref. 16 we assume identity function for scaling functions  $\mathcal{J}_S(x) \equiv x$ ,  $\mathcal{J}_P(x) \equiv x$ ,  $q(x) \equiv x$ . The distance scaling function should be an increasing function of its argument. Here, we assume the distance scaling function as

$$g(x) = 1 + x^\alpha, \quad (3)$$

what ensures non-zero values  $g(0) = 1$  of denominator for self-supportiveness in Eq. (2a).

The exponent  $\alpha$  is an arbitrary quantity which characterise the long-range interaction among actors. For small values of  $\alpha$  (for instance for  $\alpha = 2$ ) we assume good communication among actors, good access to information in the society and effective exchange of information. In contrary, for larger values of  $\alpha$  (for instance for  $\alpha = 6$ ) discussion and information exchange takes place only in the actors' nearest neighbourhood.

For  $T > 0$ , the larger the social temperature  $T$  (noise), the more often the opinions, that do not have the greatest impact are selected. As it was shown in Ref. 16 in the modelled system the phase transition occurs: below critical temperature  $T \ll T_c$  the ordered phase is observed with domination of one of the available opinion, while for  $T \gg T_c$  all opinions become equally supported by actors. Critical temperatures  $T_c$  (but for homogeneous society with  $\forall i : s_i = p_i = 0.5$ ) are  $T_c = 6.1$  and  $T_c = 4.7$ , for two and for three opinions, respectively [16]. In this article, simulations were carried out for  $T \leq 5$  to take into account different levels of noise, reaching the critical level at which agents more often take random opinions than guided by the opinion of their neighbours.

For finite values of social temperature  $T > 0$  we apply the Boltzmann choice

$$p_{i,k}(t) = \exp\left(\frac{I_{i,k}(t)}{T}\right), \quad (4a)$$

which yields probabilities

$$P_{i,k}(t) = \frac{p_{i,k}(t)}{\sum_{j=1}^K p_{i,j}(t)} \quad (4b)$$

of choosing by  $i$ -th actor in the next time step  $k$ -th opinion:

$$\xi_i(t+1) = \Xi_k, \text{ with probability } P_{i,k}(t). \quad (4c)$$

The form of dependence (4a) in statistics and economy is called logit function [11, 40].

Both, for  $T = 0$  and  $T > 0$  the calculated social impacts  $I_{i,k}(t)$  influence the  $i$ -th actor opinion  $\xi_i(t+1)$  at the subsequent time step. Newly evaluated opinions are applied synchronously to all actors. The simulations takes one thousand time steps which ensures reaching a plateau in time evolution of several observables.

The simulations are carried out on square lattice of linear size  $L = 41$  with open boundary conditions. To check the system behaviour, also simulations for  $L = 21$  and  $L = 61$  were carried out. We assume random values of supportiveness  $s_i$  and persuasiveness  $p_i$  for all actors. The studies for homogeneous society, i.e. with  $\forall i : p_i = s_i = 0.5$  were carried out in Ref. 16. The results are averaged over one hundred independent simulations with various initial distribution of opinions and actors persuasiveness and actors supportiveness.

The example of social impact calculations for a small system (with nine actors and three opinions) is given in Appendix A. The model implementation in Fortran95 [68] is attached as Listings 1 and 2 in Appendix C.

### III. RESULTS

#### A. Spatial distribution of opinions

We start presentation of our results by showing the spatial distribution of opinions for  $K = 2, 3$  (various numbers of opinions available in the system), for  $\alpha = 2, 3, 6$  (various levels of flow of information), for  $T = 0, 1, 3, 5$  (various levels of noise).

##### 1. $K = 2$

In Fig. 1 the simulation results for  $K = 2$ ,  $\alpha = 2, 3, 6$  and  $T = 0, 1, 3, 5$  are presented.

Both,  $\alpha$  (information flow) and  $T$  (noise) influence opinion formation and the spatial distribution of opinions. For  $\alpha = 2$  the consensus takes place (all actors adopt one of two opinions, except of few actors for large  $T$  values).



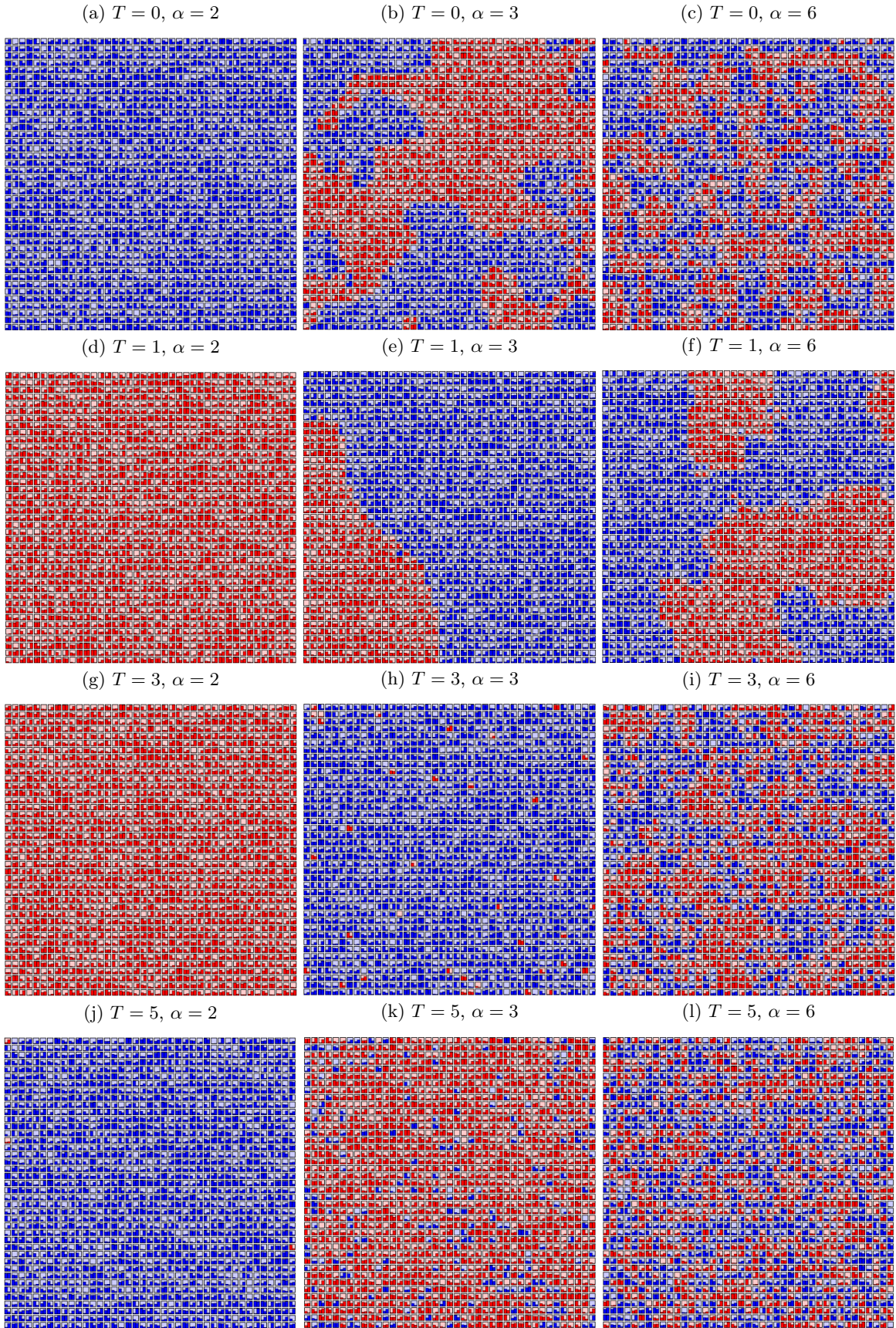


FIG. 1: Spatial distribution of opinions  $\xi$  for various values of social temperature  $T$  and exponent  $\alpha$  after  $t_{\max} = 10^3$  time steps.  $L^2 = 1681$ ,  $K = 2$ . Pictures are produced with application [69].

Interesting phenomena for  $\alpha = 3$  are observed, where the frozen initial system goes into a polarized phase of two large clusters for  $T = 1$  and into a consensus phase for  $T = 3$  (one cluster with single actors with a different opinion) before disordering for  $T = 5$ . For  $\alpha = 6$  many clusters are visible, although the introduction of noise ( $T = 1$ ) results in a more ordered system than for other  $T$  values. To sum up, the increase of  $\alpha$  and  $T$  generally causes greater disorder in the system (many clusters with both opinions), but for some values of these parameters their increase leads to order (consensus)—see Fig. 1h.

In general, we can observe four main types of structures in the formation of opinions for  $K = 2$ :

- formation of single cluster, when all agents adopt one opinion and consensus takes place (Figs. 1a, 1d, 1g, 1j),
- the majority of agents with the same opinion and single agents with opposing opinions scattered across the lattice (Fig. 1h),
- formation of several large clusters of agents with different opinions—polarisation of the group opinion (Fig. 1e),
- formation of plenty small clusters with both opinions (e.g. Figs. 1b, 1f).

## 2. $K = 3$

The simulation results for three opinions among actors (where  $K = 3$ ,  $\alpha = 2, 3, 6$  and  $T = 0, 1, 3, 5$ ) are presented in Fig. 2.

Similarly to  $K = 2$ , the formation of opinions (the formation of clusters of opinion) depends on the level of noise and the effective range of interactions among actors. For  $\alpha = 2$ , one cluster is formed—consensus take place. For  $K = 3$  the consensus among actors with three different opinions is also possible for  $\alpha = 3$ . In other cases, many clusters with three opinions or disordered system state are visible.

In general, we can observe four types of structures in the formation of opinions for  $K = 3$ , after thousand time steps:

- formation of single cluster, when all agents adopt one opinion and consensus takes place (Fig. 2a, 2d, 2g, 2j),
- the majority of agents with the same opinion and single agents with opposing opinions scattered across the lattice (Fig. 2h),
- formation of clusters with all possible opinions—polarisation of the group opinion (Fig. 2e),
- formation of plenty small clusters with all opinions (e.g. Fig. 2b, 2c, 2f).

## B. Clustering of opinions

In Figs. 1 and 2—discussed in the previous section—different phases of the system depending on the parameters  $\alpha$  and  $T$  were presented. In order to get a better look at influence of  $T$  and  $\alpha$  on system behaviour, we analyzed the histograms  $H(\mathcal{S})$  of cluster sizes  $\mathcal{S}$  after thousand steps of simulation gathered from hundred simulations (see Figs. 3, 4).

We apply the Hoshen–Kopelman algorithm [70] for clusters detection. In Hoshen–Kopelman algorithm each actor is labelled in such way, that actors with the same opinions and in the same cluster have identical labels. The algorithm allows for cluster detection in multi-dimensional space and for complex neighbourhoods [71–75], here however, we assume the simplest case, i.e. square lattice with von Neumann neighbourhood (see Fig. 5).

To better explain the phenomena observed in Figs. 3 and 4, the following parameters describing the number and size of clusters were selected:

- average largest cluster size  $\langle \mathcal{S}_{\max} \rangle$ ,
- average cluster number  $\langle n_c \rangle$ ,
- average number of small clusters  $\langle n_s \rangle$ .

The example of clusters

- size distribution counting (for preparation histograms  $H(\mathcal{S})$  for Figs. 3 and 4),
- average largest value  $\langle \mathcal{S}_{\max} \rangle$  (for Figs. 6a, 7a),



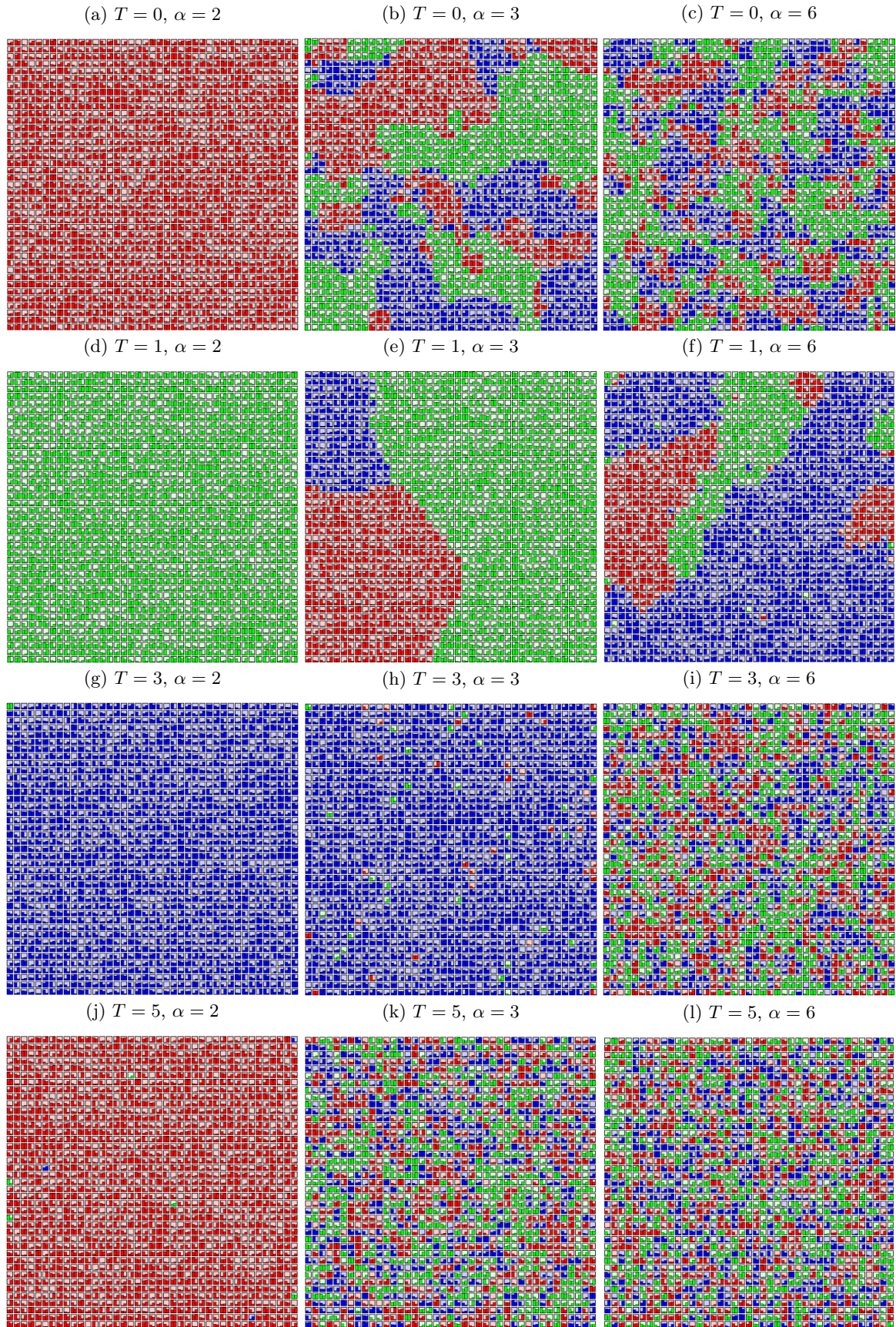


FIG. 2: Spatial distribution of opinions  $\xi$  for various values of social temperature  $T$  and exponent  $\alpha$  after  $t_{\max} = 10^3$  time steps.  $L^2 = 1681$ ,  $K = 3$ . Pictures are produced with application [69].

- and average numbers  $\langle n_c \rangle$  (for Figs. 6b, 7b) and  $\langle n_s \rangle$  (for Figs. 6c, 7c)

are provided in Appendix B.

On the left panels of Fig. 6 (for  $K = 2$ ) and Fig. 7 (for  $K = 3$ ) the ‘heat maps’ and numerical values of  $\langle \mathcal{S}_{\max} \rangle$ ,  $\langle n_c \rangle$  and  $\langle n_s \rangle$  for different values of  $\alpha$  and  $T$  are presented. The supplementary ‘contour maps’, presenting the same data but allowing for better visualisation of non-monotous character of these data, are included on the right panels of these figures. On left panels average values of the largest cluster sizes  $\langle \mathcal{S}_{\max} \rangle$  are expressed as a fraction of the number of sites ( $L^2$ ). The results were averaged over hundred simulations and gathered after  $t_{\max} = 1000$  time steps.

As can be seen in Figs. 3, 4, the shapes of histograms are very similar to each other for  $K = 2$  (Fig. 3) and  $K = 3$  (Fig. 4). In both cases, there are clear differences in the shape of histograms due to values of  $\alpha$  (information flow, effective range of interaction among actors):

- For  $\alpha = 1$  and  $\alpha = 2$ —where the effective range of interaction is the largest—the unanimity of opinions is achieved (in the case of  $\alpha = 2$ , single agents and rarely small clusters with opposite opinions may appear).
- The most interesting are the histograms for  $\alpha = 3$  (see figures forming columns from 3c to 3w and from 4c to 4w), because the difference in the shape of histograms due to noise ( $T$ ) is also visible. For  $\alpha = 3$ , various phases in the system behaviour are observed. The system from the disordered state, with the growth of  $T$  is increasingly ordered. As  $T$  increases, more and more clusters appear close to the maximum cluster size in this lattice and more and more small clusters consisting of single agents.
- For  $\alpha = 6$ , histograms have similar shapes for all  $T$  values and they indicate the phase of system disorder (a large number of clusters), apart from slight orderliness for  $T = 1$  (see Figs. 3h and 4h).

In Figs. 3 and 4, we can also notice that for  $\alpha > 2$ , the greater the randomness in adopting opinions by agents (greater  $T$ ), the more single clusters containing one agent and several agents appear.

### 1. $K = 2$

As can be seen in Fig. 6a, the average size of the maximum cluster  $\langle \mathcal{S}_{\max} \rangle$  decreases with  $\alpha$  for fixed  $T$  values. The appearance of noise in the system ( $T = 1$ ) slightly organizes the system in relation to the noiseless situation with  $T = 0$  (see Fig. 6a). Indeed, like in earlier studies [64, 66], small level of noise brought more order to the system. In addition, the introduction of noise ( $T$ ) in the adoption of opinions causes an increase in  $\langle \mathcal{S}_{\max} \rangle$ , and then its decrease, which is especially visible for  $\alpha > 2$ . The presense of noise  $T > 0$  results in greater orderliness of the system but only up to certain  $T$  values. Particularly interesting are the large values of  $\langle \mathcal{S}_{\max} \rangle$  for  $\alpha = 3$  and  $T = 2, 3, 4$ . This issue will be discussed below.

Figure 6b shows the simulation results of the average number of clusters  $\langle n_c \rangle$ . As can be seen, for fixed noise level  $T$ , the average number of clusters  $\langle n_c \rangle$  increases with  $\alpha$ . This figure also shows that for  $\alpha \geq 3$  the average number of clusters increases with  $T$ . In addition, comparing the results for all  $\alpha$  values and for the noiseless system ( $T = 0$ ) with the results for small noise level ( $T = 1$ ), it can be seen that the introduction of noise results in system ordering.

The average number of small clusters  $\langle n_s \rangle$  increases with  $\alpha$  for fixed values of  $T$  (see Fig. 6c). For  $\alpha = 1$  there are no small clusters, and for  $\alpha = 2$  there are few of them. The increase in the number of small clusters due to  $T$  and  $\alpha$  is well visible for  $\alpha \geq 2$ , i.e. when the range of interaction between agents is small.

Considering all results presented in Fig. 6 we can notice, that:

- For  $\alpha \leq 2$  we observe the system phase in which there is a consensus (one large cluster representing actors sharing one of the available opinions). The average size of the largest cluster is equal to the size of the lattice. For  $\alpha = 2$  and  $T > 2$ , the average number of clusters is larger than one, but these higher  $\langle n_c \rangle$  values only mean the appearance of clusters consisting of single agents, as  $|\langle n_c \rangle - \langle n_s \rangle| \approx 1$ , which is shown in Figs. 6b and 6c and also visible in Figs. 3n, 3r, and 3v.
- An interesting phenomenon can be observed for  $\alpha = 3$ , where the frozen noiseless system goes into a more ordered phase for  $T = 1$  and  $T = 2$ , and into a consensus phase for  $T = 3$  before disordering at  $T = 5$  (see. Fig. 6). Polarization of opinion is observed for  $T = 1$  (about 60% of simulations end with polarization and about 40% of them end with consensus). The average size of the largest cluster contains 83.1% of all agents on the lattice. The average number of clusters is very small and it equals 1.9, and the average number of small clusters is 0.17, which means that the simulations mostly end in a state containing two clusters, one of which is definitely larger than the other. This is also visible in Figs. 1 and 3g. For  $T = 2$ , more and more system ordering is observed (more and more simulations end with unanimity).



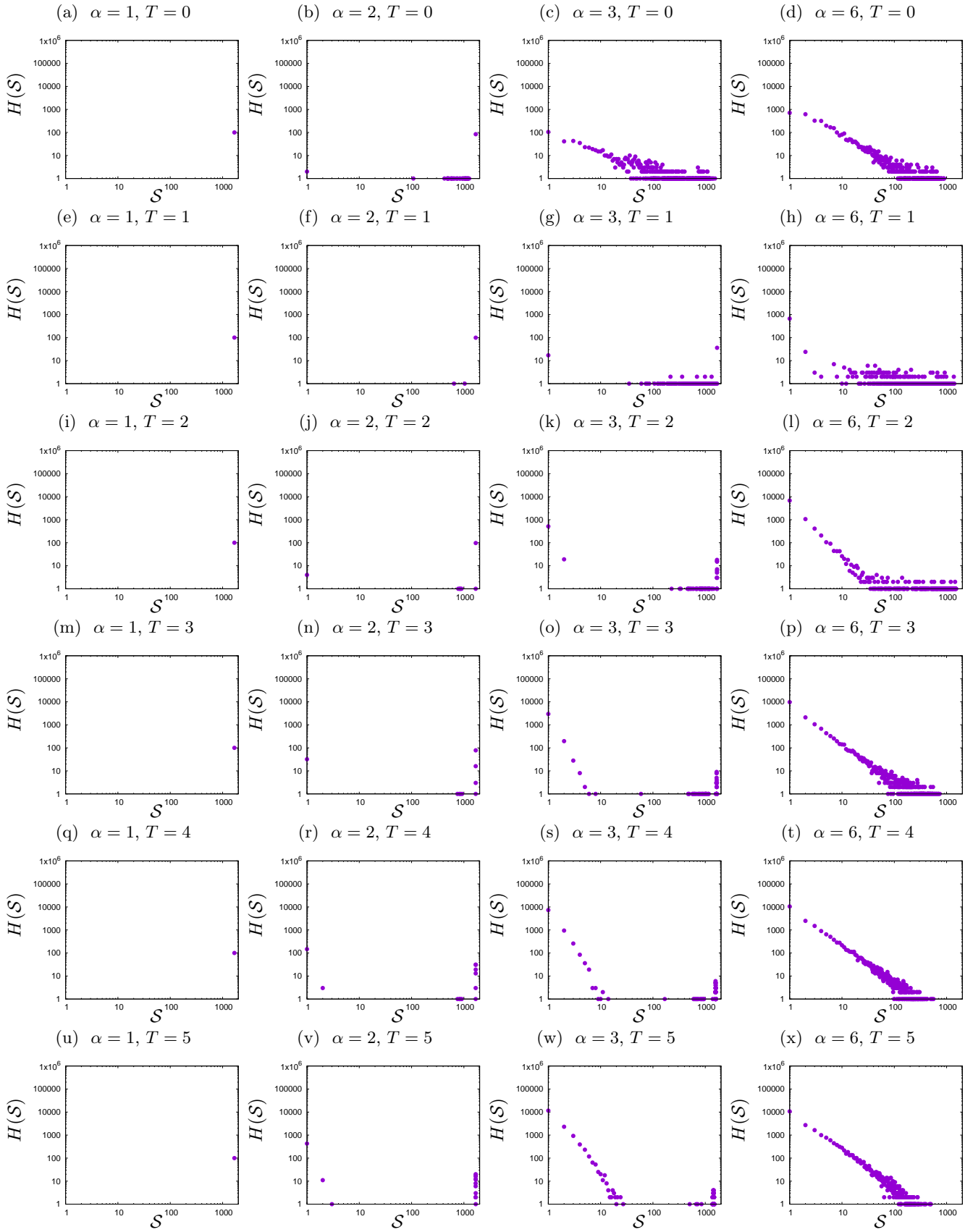


FIG. 3: Histograms  $H(S)$  of cluster sizes  $S$  for various values of social temperature  $T$  and exponent  $\alpha$ .  $L = 41$ ,  $K = 2$ . The results are gathered from hundred runings with different initial conditions after  $t_{\max} = 1000$  time steps.

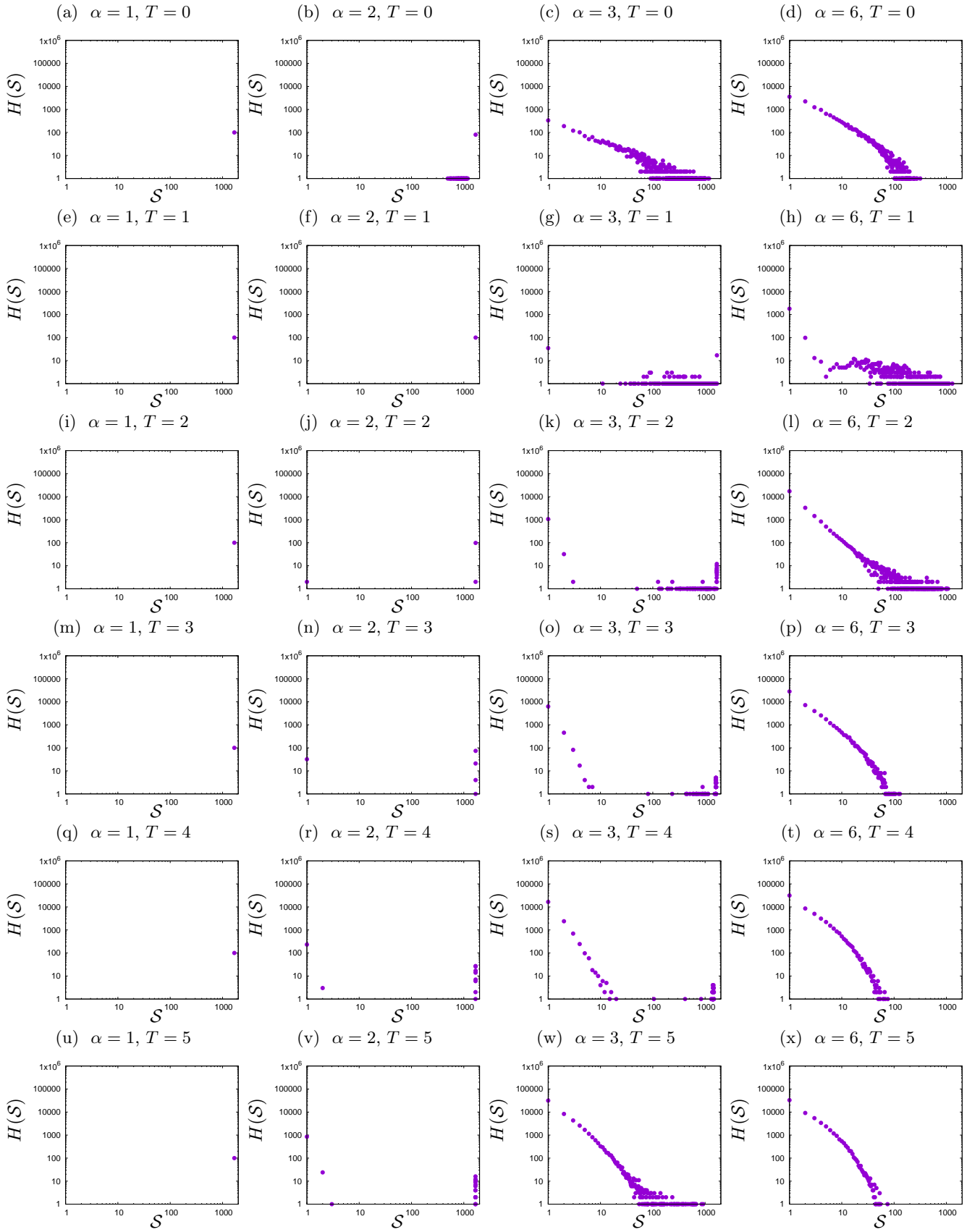


FIG. 4: Histogram  $H(S)$  of cluster sizes  $S$  for various values of social temperature  $T$  and exponent  $\alpha$ .  $L = 41$ ,  $K = 3$ . The results are gathered from hundred runings with different initial conditions after  $t_{\max} = 1000$  time steps.

The second phase in the case of  $\alpha = 3$  takes place for  $T = 3$ . Despite the high values of noise  $T$ , the size of the maximum cluster  $\langle \mathcal{S}_{\max} \rangle$  is still very large and contains about 90% of all actors (Fig. 6a), and the average number of clusters is definitely larger than for  $T \leq 2$  (see Fig. 6b). An increase in noise level surprisingly causes a kind of order. In this case, one of the opinions dominates, but representatives of the opposite opinion appear in the form of small individual clusters. The average number of small clusters  $\langle n_s \rangle$  is 32 for  $T = 3$ . This number when compared to the average number of clusters  $\langle n_c \rangle$  in Fig. 6b (33.2 for  $T = 3$ ) indicates the emergence of one large cluster and individual small clusters (the average number of small clusters  $\langle n_s \rangle$  differs by approximately one from the average number of clusters  $\langle n_c \rangle$ ). This means, that system evolution toward unanimity of opinion dominates system dynamics for  $T = 3$ .

- For  $T = 4$ , the size of the largest cluster  $\langle \mathcal{S}_{\max} \rangle$  is still very large (and reaches ca. 90% of all actors), but although  $\langle n_c \rangle$  differs from  $\langle n_s \rangle$  by about one, both the number of clusters and the number of small clusters are definitely larger than in the case of  $T = 3$  (Fig. 6). So, for  $T = 4$ , the system goes into a disordered phase.

In the case of  $T = 5$ , the system enters a phase of disorder, because there are definitely more clusters with opposite opinions and they have a larger size than for  $T = 3$  and  $T = 4$ , which is also visible in Fig. 3w and Fig. 1.

For  $\alpha = 4$  and  $\alpha = 5$ , when the noise level goes to  $T = 2$ , a slight increase of noise induces more order (see Figs. 6 and 3). This can be seen in the average size of the largest cluster ( $\langle \mathcal{S}_{\max} \rangle$  for  $T = 2$  is larger than for  $T = 1$ ) and by comparing the average number of clusters  $\langle n_c \rangle$  with the average number of small clusters  $\langle n_s \rangle$  (the difference is smaller than for  $T = 1$ )—Fig. 6.

When the interaction effectively takes place only among the nearest neighbors (for  $\alpha = 6$ ), this effect vanishes.

To check the system behaviour for  $K = 2$ , simulations for  $L = 21$  and  $L = 61$  were also carried out. The simulations for the smaller and larger network of agents showed results consistent with the presented for networks with size  $L = 41$ . Slight differences were observed for  $\alpha = 3$ , where for  $T = 1$  and  $T = 2$  after 1000 steps of simulation, in the case of a smaller network, consensus is more often observed, and for a larger network less often.

To sum up, three main types of structures in the formation of opinions for  $K = 2$  are observed:

- formation of single cluster, when all agents adopt one opinion and consensus takes place (for  $\alpha \leq 2$ ,  $T = 1, 2, 3, 4, 5$  and  $\alpha = 3$ ,  $T = 2, 3, 4$ ),
- greater orderliness—polarization of opinions in clusters ( $\alpha = 3$ ,  $T = 1, T = 2$  and for  $\alpha = 3, 4$ , and  $T = 2$ ),
- formation of plenty small clusters with both opinions—disorder (for other values of  $\alpha$  and  $T$ ).

## 2. $K = 3$

In Fig. 7 the simulation results for  $K = 3$  are presented. The average size of the largest cluster  $\langle \mathcal{S}_{\max} \rangle$  (Fig. 7a) decreases with  $\alpha$  for fixed values of the noise level  $T$ , as it was observed for  $K = 2$ . For  $\alpha = 1$  and  $\alpha = 2$ ,  $\langle \mathcal{S}_{\max} \rangle$  is equal to the number of all actors on the lattice. For  $\alpha > 2$ , the average size of the largest cluster  $\langle \mathcal{S}_{\max} \rangle$  increases up to a certain value of  $T$ , and then decreases. This inflection point is nearly  $T = 2$ .

In the case of the average number of clusters  $\langle n_c \rangle$ —which is presented in Fig. 7b—this number is the smallest for  $T = 1$ , i.e. as soon as noise is introduced to the system. Similarly to the case of  $K = 2$ , for fixed noise level  $T$ , the average number of clusters  $\langle n_c \rangle$  increases with  $\alpha$ . Fig. 7b also shows, that for  $\alpha > 2$  the average number of clusters  $\langle n_c \rangle$  increases with  $T$  for all  $T > 1$ .

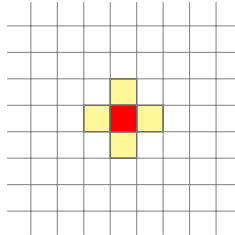


FIG. 5: The actors with identical opinions  $\Xi_k$  belong to the common cluster if they are in von Neumann neighbourhood.



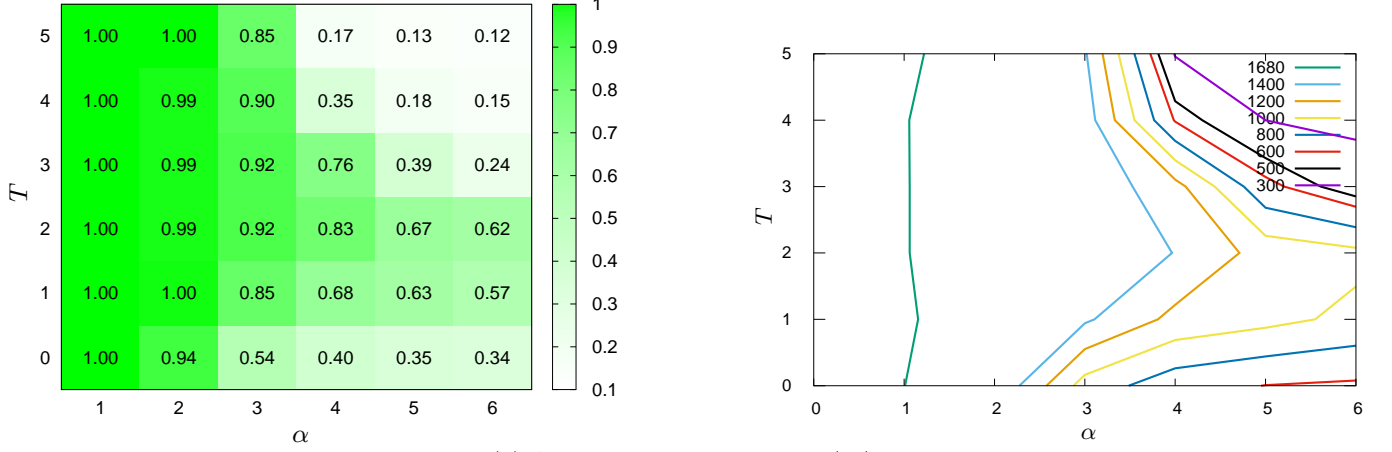
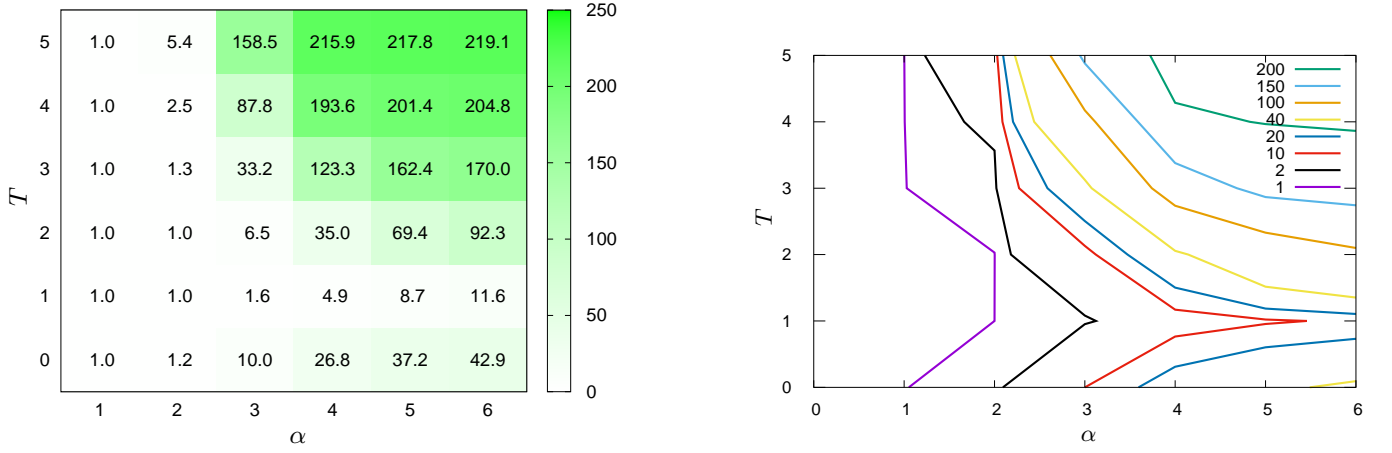
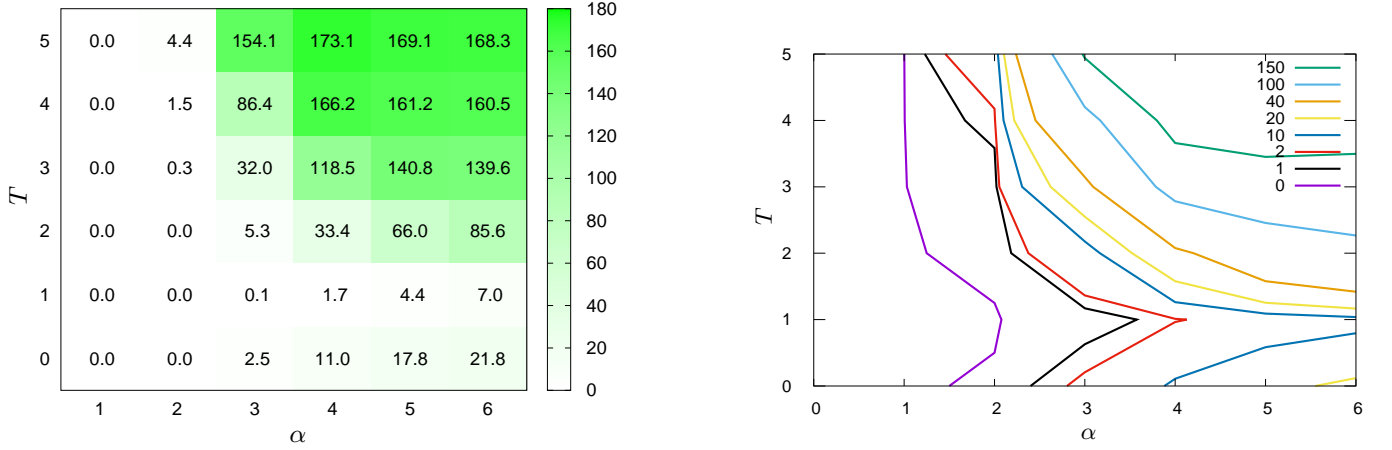
(a) Average largest cluster size  $\langle \mathcal{S}_{\max} \rangle$  (in left panel normalized to  $L^2$ ).(b) Average number of clusters  $\langle n_c \rangle$ .(c) Average number of small cluster  $\langle n_s \rangle$ .

FIG. 6: Average (a) largest cluster size  $\langle \mathcal{S}_{\max} \rangle$ , (b) number of clusters  $\langle n_c \rangle$  and (c) average number of small clusters  $\langle n_s \rangle$  for various values of noise level  $T$  and exponent  $\alpha$ .  $L^2 = 1681$ ,  $K = 2$ . The results are averaged over hundred runings with different initial conditions and measured after  $t_{\max} = 10^3$  time steps.

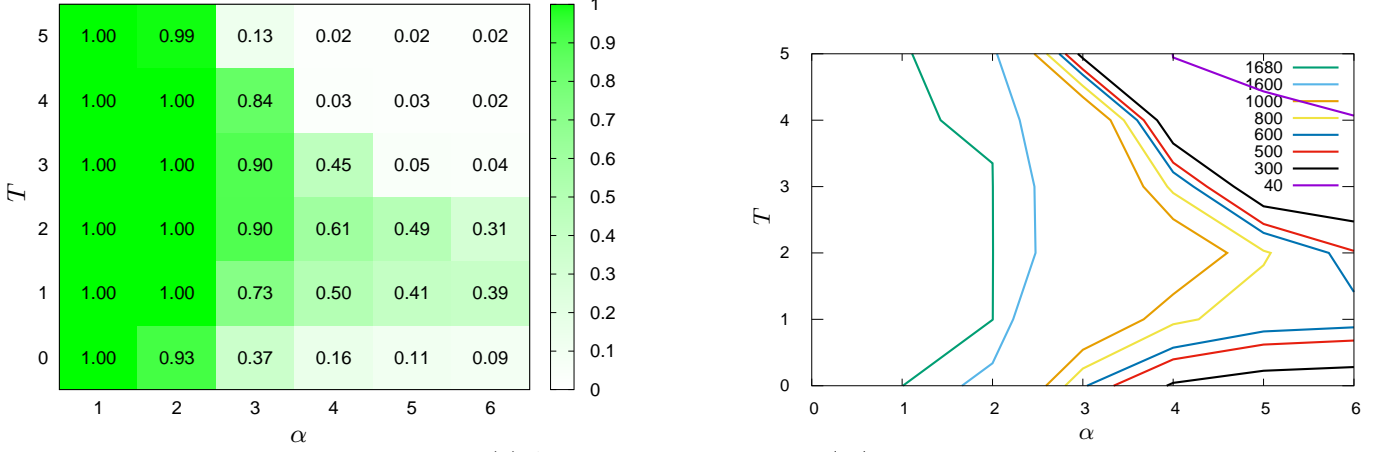
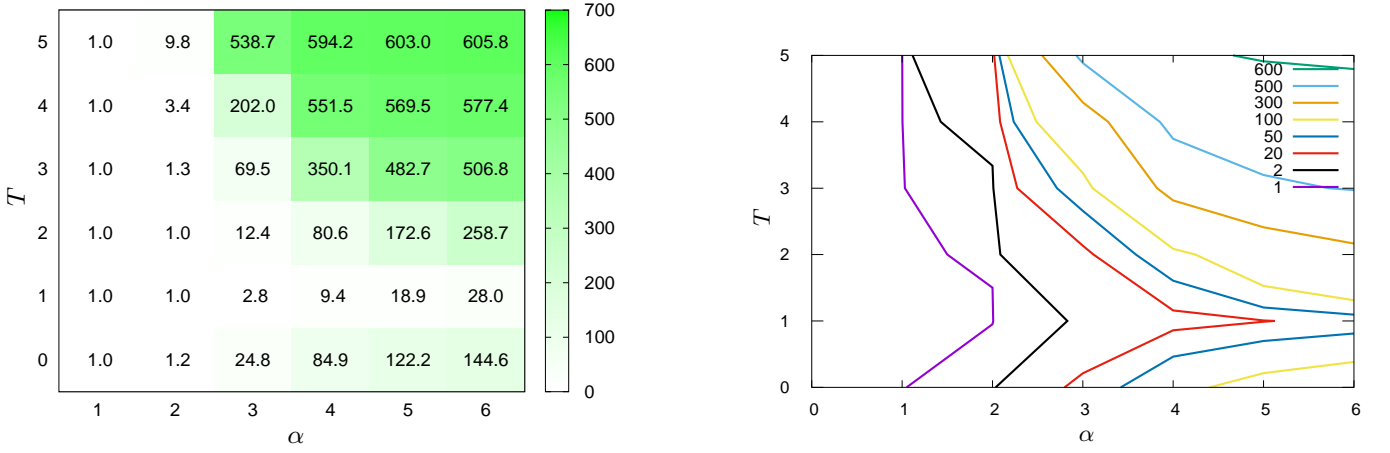
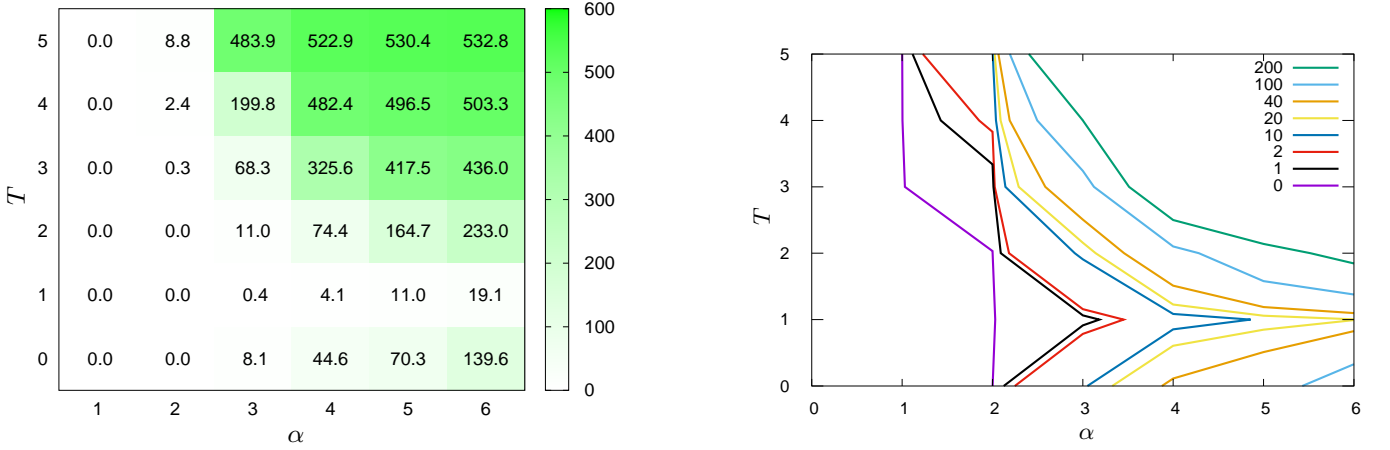
(a) Average largest cluster size  $\langle S_{\max} \rangle$  (in left panel normalized to  $L^2$ ).(b) Average number of clusters  $\langle n_c \rangle$ .(c) Average number of small cluster  $\langle n_s \rangle$ .

FIG. 7: Average (a) largest cluster size  $\langle S_{\max} \rangle$ , (b) number of clusters  $\langle n_c \rangle$  and (c) average number of small clusters  $\langle n_s \rangle$  for various values of noise level  $T$  and exponent  $\alpha$ .  $L^2 = 1681$ ,  $K = 3$ . The results are averaged over hundred runings with different initial conditions and measured after  $t_{\max} = 10^3$  time steps.

The average number of small clusters  $\langle n_s \rangle$ , similarly to the case of  $K = 2$ , increases with the increase  $T$  and  $\alpha$  (Fig. 7c). For  $\alpha = 1$  there are no small clusters, and for  $\alpha = 2$  they appear only for  $T > 3$ . The increase in the number of small clusters  $\langle n_s \rangle$  with increase of  $T$  and  $\alpha$  is clearly visible for  $\alpha > 2$ .

As the simulation results suggest—also in the case of  $K = 3$  opinions available in the system—various phases in the system behaviour can be observed. These phases are induced by interplay of noise level  $T$  and effective range of interaction among actors  $\alpha$ . First of all, for  $\alpha = 1$  and all  $T$  values, a large cluster with one opinion is formed (consensus takes place). In this case,  $\langle \mathcal{S}_{\max} \rangle$  are equal to the number of all agents on the lattice, and the average number of clusters  $\langle n_c \rangle$  is one (see Figs. 7a, 7b—left panels). Single cluster is also created in the case of  $\alpha = 2$ . As can be seen in Figs. 7a and 7b the average largest cluster size is close to the system size  $\langle \mathcal{S}_{\max} \rangle \approx L^2$ , and the average number of clusters is close to one  $\langle n_c \rangle \approx 1$ . The exceptions occur for large values of the noise level  $T \geq 4$ , but this is associated with the appearance of single small and short-living clusters, which is typical for high randomness in actors behaviour. In this situation the average number of small clusters differs by approximately one from the average number of clusters  $|\langle n_c \rangle - \langle n_s \rangle| \leq 1$ . These results are confirmed by the data in Figs. 7b and 7c.

As in the case of two opinions ( $K = 2$ ), interesting phenomena are visible for  $\alpha = 3$ . For  $T = 1$ , polarization of opinions is observed. In 80% of cases of the final system state two or three clusters of opinions are created, one of which is larger than the others ( $\mathcal{S}_{\max}/L^2 = 0.73$ , see Fig. 2e). For  $T = 2$ , as in the case of two opinions, more ordering is observed than for  $T = 1$ . Consequently, by increasing noise level, for  $T = 3$  a consensus takes place (one large cluster and small clusters with only single actor). The average size of the largest cluster is still very large and contains about 90% of all actors in the lattice. Although the average number of clusters  $\langle n_c \rangle$  is quite large, when compared with the average number of small clusters  $\langle n_s \rangle$  it indicates the existence of one large cluster and single small clusters (the average number of clusters differs by approximately one from the average number of small clusters  $|\langle n_c \rangle - \langle n_s \rangle| \approx 1$ —see Figs. 7b and 7c). For  $\alpha = 3$  and  $T = 4$ , despite the still high  $\langle \mathcal{S}_{\max} \rangle$ , the number of small clusters increases, which leads to a disorder phase for  $T = 5$ . The difference between average number of clusters  $\langle n_c \rangle$  and average number of small clusters  $\langle n_s \rangle$  is definitely greater than one cluster  $|\langle n_c \rangle - \langle n_s \rangle| \gg 1$  (cf. Figs. 7a, 7b).

For  $\alpha > 3$  and all  $T$  values, system disorder (many clusters of all opinions) is visible—Figs. 2 and 4, with the exception of  $\alpha = 4$  and  $\alpha = 5$ , when a slight increase of noise ( $T = 2$ ) does induce more order than for  $T = 1$  (see Figs. 7 and 4). As for  $K = 2$ , in the case of three opinions, simulations for  $L = 21$  and  $L = 61$  were also carried out. The simulations for the smaller and larger network of agents showed similar results to the presented for networks with size  $L = 41$ . Slight differences were observed for  $\alpha = 3$ , and  $T = 1$  and  $T = 2$  after 1000 steps of simulation, where ordering in clusters is more visible in small networks than in large ones.

To sum up, we can notice three main phases in the behaviour of the model for  $K = 3$ :

- formation of single cluster, when all agents adopt one opinion and consensus takes place (for  $\alpha \leq 2$ ;  $T = 1, 2, 3, 4, 5$  and  $\alpha = 3, T = 3$ ),
- greater orderliness—polarization of opinions in clusters (sometimes one cluster or ordering opinions in two or three clusters, where two or three opinions occur ( $\alpha = 3, T = 1, T = 2$  and for  $\alpha = 3, 4, T = 2$ ),
- formation of plenty clusters with all three opinions—disorder (for other values of  $\alpha$  and  $T$ ).

#### IV. SUMMARY AND CONCLUSIONS

In this paper, we are interested in how opinions are formed and how they spread in the community. We were investigating how flow of information in the community and randomness of human behaviour influence formation of opinions, its spreading and its polarisation. The community was presented as a square lattice of linear size  $L$  with open boundary conditions, which is fully filled by actors.

The flow of information was controlled by the parameter  $\alpha$ . This parameter reflects the effective impact of the neighbourhood on the opinion of the actors. In case of low values of this parameter, actors shape their opinion basing on a large number of actors (including distant neighbours). In our research, we also take into account the randomness in adopting opinions, which is expressed in the noise parameter  $T$ . The larger  $T$ , the more often actors adopt opinions which have no greatest impact on them

Each actor in our model is characterised, in addition to the opinion, by two parameters. They are the intensity of persuasion ( $p_i$ ) and the intensity of support ( $s_i$ ). The higher the value of persuasiveness  $p_i$ , the actor more easier convincing other actors to accept his/her opinion. With bigger ( $s_i$ ), the agent convinces more strongly other actors. These parameters therefore determine the effectiveness of which an individual may interact with or influence other individuals by changing or confirming their opinions. In all performed simulations, we adopted random values of ( $p_i$ ) and ( $s_i$ ) parameters, which brings us closer to the social reality, in which we do not usually have data on the strength with which the unit affects other units. Simulations have been carried out when actors have a choice of two



or three opinions on a given topic. First, the spatial distribution of opinions after thousand steps of simulation was analysed. The simulations showed how clusters of opinion are formed depending on (i) the flow of information in the agents' network, and (ii) the randomness in forming the opinion. For both  $K = 2$  and  $K = 3$  we can see consensus, polarization of opinions and the formation of many clusters of available opinions.

As it was shown in previous sections, the clustering of opinions is influenced by both the level of randomness in actors' decisions (noise) and the impact coming from neighbours. Generally, the size of the largest cluster of opinions decreases with the increase of  $\alpha$  (as can be seen by inspection of columns in Figs. 1 and 2). Furthermore, the number of clusters for both  $K = 2$  and  $K = 3$  increases with  $\alpha$ , i.e. the smaller effective range of actors' interaction the more difficult forming clusters of opinions. Intuitively, an increase in the number of clusters with an increase in noise level  $T$  is expected. In fact, the number of clusters is growing, but for  $\alpha = 3$  and  $T = 3$  we have one cluster and single agents with opposite opinions, as can be seen in Figs. 1 and 2. In this case, introducing of noise ( $T$ ) leads to consensus with single representatives of the opposite opinion(s). In addition, for  $\alpha \geq 3$ , a slight increase of noise level ( $T = 2$ ) induces more order than for  $T = 1$  (with the exception for  $\alpha = 6$  when the interaction effectively takes place only among the nearest neighbors).

In summary, the simulations showed that opinion formation and spread is influenced by both: efficiency of information flow among actors and noise level. Better information flow, i.e. better contacts among actors facilitates the spread of opinion and its formation. In the case of small values of  $\alpha$  (when information flow is very good) the unanimity of opinion is reached and consensus takes place, as in most sociophysical models of opinion dynamics [38], for both, two and three opinions available in the system. For large values of  $\alpha$ —when effectively only the nearest neighbours exert impact on given actor—the polarisation of opinions is weak and there are many small groups of actors with the same opinion.

The lack of consensus in models is mainly caused by the introduction of noise [76] or anti-conformism [77]. In the presented model there is no global agreement also for  $T = 0$  (when there is no noise). For  $T = 0$  and  $\alpha \geq 3$  clusters of both opinions (or three for  $K = 3$ ) appear. In addition, in the presented model, noise for certain values of  $\alpha$  promotes unanimity. This situation occurs for  $\alpha = 3$  (both for  $K = 2$  and  $K = 3$ ), when the system from the frozen state, with increasing noise  $T$ , achieves the consensus state for  $T = 3$ , before disordering for  $T = 5$ .

As it was mentioned earlier, many studies indicate irrationality and unpredictability in the process of forming opinions [9–13]. As our simulations have shown, this randomness in adopting opinions (noise) plays a crucial role. A low level of noise (low  $T$  values) results in less clusters of opinion than in the absence of noise ( $T = 0$ ). However, the most interesting is the fact, that the high noise levels ( $T = 2, 3, 4$ ) results in a more ordered system than for small values of noise  $T$  (this is the case with  $\alpha = 3$ ). Thus, noise favours consensus and polarization of opinion in groups, but only when the influence of distant neighbours is significant. If the exchange of opinions takes place only with the nearest neighbors, this effect is not observed.

In future research, we intend to take into account the impact of strong leaders on the opinion dynamics. Also the influence of external sources of information (for instance the impact of mass media) is worth of investigation.

## ACKNOWLEDGMENTS

We are grateful to anonymous Referee for his/her valuable comments which greatly improved the current version of manuscript. This research was supported by the National Science Centre (NCN) in Poland (grant no. UMO-2014/15/B/HS4/04433) and PL-Grid infrastructure.

- 
- [1] D. Acemoglu and A. Ozdaglar, “Opinion dynamics and learning in social networks,” *Dynamic Games and Applications* **1**, 3–49 (2011).
  - [2] M. O. Jackson and L. Yariv, “Diffusion, strategic interaction, and social structure,” (North-Holland, 2011) pp. 645–678.
  - [3] T. Duncan and S. E. Moriarty, “A communication-based marketing model for managing relationships,” *Journal of Marketing* **62**, 1–13 (1998).
  - [4] H. A. Simon, “A behavioral model of rational choice,” *The Quarterly Journal of Economics* **69**, 99–118 (1955).
  - [5] R. A. Bentley, P. Ormerod, and M. Batty, “Evolving social influence in large populations,” *Behavioral Ecology and Sociobiology* **65**, 537–546 (2011).
  - [6] K. Kułakowski, P. Kulczycki, K. Misztal, A. Dydejczyk, P. Gronek, and M. J. Krawczyk, “Naming boys after U.S. presidents in 20th century,” *Acta Physica Polonica A* **129**, 1038–1044 (2016).
  - [7] M. J. Krawczyk, A. Dydejczyk, and K. Kułakowski, “The Simmel effect and babies' names,” *Physica A* **395**, 384–391 (2014).
  - [8] M. E. Guffy, K. Rhoddes, and P. Rogin, *Business Communication* (South-Western, Toronto, 2005).

- [9] A. Kowalska-Pyzalska, K. Maciejowska, K. Sznajd-Weron, and R. Weron, “Modeling consumer opinions towards dynamic pricing: An agent-based approach,” in *11th International Conference on the European Energy Market* (2014) pp. 1–5.
- [10] A. Kowalska-Pyzalska, K. Maciejowska, K. Suszczyński, K. Sznajd-Weron, and R. Weron, “Turning green: Agent-based modeling of the adoption of dynamic electricity tariffs,” *Energy Policy* **72**, 164–174 (2014).
- [11] K. Byrka, A. Jędrzejewski, K. Sznajd-Weron, and R. Weron, “Difficulty is critical: The importance of social factors in modeling diffusion of green products and practices,” *Renewable and Sustainable Energy Reviews* **62**, 723–735 (2016).
- [12] D. Stadelmann and B. Torgler, “Bounded rationality and voting decisions over 160 years: Voter behavior and increasing complexity in decision-making,” *PLoS ONE* **8**, e84078 (2013).
- [13] P. Sobkowicz, “Opinion dynamics model based on cognitive biases of complex agents,” *JASSS—the Journal of Artificial Societies and Social Simulation* **21**, (4)8 (2018).
- [14] A. Apolloni and F. Gargiulo, “Diffusion processes through social groups’ dynamics,” *Advances in Complex Systems* **14**, 151–167 (2011).
- [15] B. Latané, “The psychology of social impact,” *American Psychologist* **36**, 343–356 (1981).
- [16] P. Bańcerowski and K. Malarz, “Multi-choice opinion dynamics model based on Latané theory,” *European Physical Journal B* **92**, 219 (2019).
- [17] P. Bańcerowski, Master’s thesis, AGH University of Science and Technology, Kraków (2017), in Polish.
- [18] B. Latané and S. Harkins, “Cross-modality matches suggest anticipated stage fright a multiplicative power function of audience size and status,” *Perception & Psychophysics* **20**, 482–488 (1976).
- [19] J. M. Darley and B. Latané, “Bystander intervention in emergencies—Diffusion of responsibility,” *Journal of Personality and Social Psychology* **8**, 377–383 (1968).
- [20] B. Latané and S. Nida, “Ten years of research on group size and helping,” *Psychological Bulletin* **89**, 308–324 (1981).
- [21] A. Nowak, J. Szamrej, and B. Latané, “From private attitude to public opinion: A dynamic theory of social impact,” *Psychological Review* **97**, 362–376 (1990).
- [22] E. Burgos, L. Hernández, H. Ceva, and R. P. J. Perazzo, “Entropic determination of the phase transition in a coevolving opinion-formation model,” *Physical Review E* **91**, 032808 (2015).
- [23] P. Holme and M. E. J. Newman, “Nonequilibrium phase transition in the coevolution of networks and opinions,” *Physical Review E* **74**, 056108 (2006).
- [24] A. C. R. Martins, “Discrete opinion dynamics with  $M$  choices,” (2019), [arXiv:1905.10878 \[physics.soc-ph\]](https://arxiv.org/abs/1905.10878).
- [25] Degang Wu and Kwok Yip Szeto, “Analysis of timescale to consensus in voting dynamics with more than two options,” *Physical Review E* **97**, 042320 (2018).
- [26] S. Galam, “The drastic outcomes from voting alliances in three-party democratic voting (1990–2013),” *Journal of Statistical Physics* **151**, 46–68 (2013).
- [27] K. Malarz and K. Kułakowski, “Indifferents as an interface between contra and pro,” *Acta Physica Polonica A* **117**, 695–699 (2010).
- [28] S. Gekle, L. Peliti, and S. Galam, “Opinion dynamics in a three-choice system,” *European Physical Journal B* **45**, 569–575 (2005).
- [29] M. S. de la Lama, I. G. Szendro, J. R. Iglesias, and H. S. Wio, “Van Kampen’s expansion approach in an opinion formation model,” *European Physical Journal B* **51**, 435–442 (2006).
- [30] F. Vazquez and S. Redner, “Ultimate fate of constrained voters,” *Journal of Physics A—Mathematical and General* **37**, 8479–8494 (2004).
- [31] S. Galam, “Political paradoxes of majority-rule voting and hierarchical systems,” *International Journal of General Systems* **18**, 191–200 (1991).
- [32] S. Galam, “Social paradoxes of majority-rule voting and renormalization-group,” *Journal of Statistical Physics* **61**, 943–951 (1990).
- [33] R. Axelrod, “The dissemination of culture: A model with local convergence and global polarization,” *Journal of Conflict Resolution* **41**, 203–226 (1997).
- [34] C. Weimer, J. O. Miller, R. Hill, and D. Hodson, “Agent scheduling in opinion dynamics: A taxonomy and comparison using generalized models,” *JASSS—the Journal of Artificial Societies and Social Simulation* **22**, (4)5 (2019).
- [35] M. J. Krawczyk and K. Kułakowski, “On a combinatorial aspect of fashion,” *Acta Physica Polonica A* **123**, 560–563 (2013).
- [36] K. Sznajd-Weron and J. Sznajd, “Who is left, who is right?” *Physica A* **351**, 593–604 (2005).
- [37] A. Sirbu, V. Loreto, V. D. P. Servedio, and F. Tria, “Opinion dynamics: Models, extensions and external effects,” in *Participatory Sensing, Opinions and Collective Awareness*, edited by V. Loreto, M. Haklay, A. Hotho, V. D. P. Servedio, G. Stumme, J. Theunis, and F. Tria (Springer International Publishing, Cham, 2017) pp. 363–401.
- [38] C. Castellano, S. Fortunato, and V. Loreto, “Statistical physics of social dynamics,” *Reviews of Modern Physics* **81**, 591–646 (2009).
- [39] D. Stauffer, “Opinion dynamics and sociophysics,” in *Encyclopedia of Complexity and Systems Science*, edited by R. A. Meyers (Springer, New York, NY, 2009) pp. 6380–6388.
- [40] S. P. Anderson, A. De Palma, and J. F. Thisse, *Discrete Choice Theory of Product Differentiation* (MIT Press, Cambridge, MA, 1992).
- [41] S. Galam, “Sociophysics: A review of Galam models,” *International Journal of Modern Physics C* **19**, 409–440 (2008).
- [42] K. Malarz and K. Kułakowski, “The Sznajd dynamics on a directed clustered network,” *Acta Physica Polonica A* **114**, 581–588 (2008).
- [43] F. Slanina, K. Sznajd-Weron, and P. Przybyła, “Some new results on one-dimensional outflow dynamics,” *EPL* **82**, 18006 (2008).

- [44] K. Sznajd-Weron, “Sznajd model and its applications,” *Acta Physica Polonica B* **36**, 2537–2547 (2005).
- [45] K. Sznajd-Weron and J. Sznajd, “Opinion evolution in closed community,” *International Journal of Modern Physics C* **11**, 1157–1165 (2000).
- [46] F. Gargiulo and Y. Gandica, “The role of homophily in the emergence of opinion controversies,” *JASSS—the Journal of Artificial Societies and Social Simulation* **20**, (3)8 (2017).
- [47] J.-D. Mathias, S. Huet, and G. Deffuant, “Bounded confidence model with fixed uncertainties and extremists: The opinions can keep fluctuating indefinitely,” *JASSS—the Journal of Artificial Societies and Social Simulation* **19**, (1)6 (2016).
- [48] K. Malarz and K. Kułakowski, “Mental ability and common sense in an artificial society,” *Europhysics News* **45**, 21–23 (2014).
- [49] K. Malarz and K. Kułakowski, “Bounded confidence model: addressed information maintain diversity of opinions,” *Acta Physica Polonica A* **121**, B86–B88 (2012).
- [50] K. Malarz, P. Gronek, and K. Kułakowski, “Zaller–Deffuant model of mass opinion,” *JASSS—the Journal of Artificial Societies and Social Simulation* **14**, (1)2 (2011).
- [51] K. Kułakowski, “Opinion polarization in the receipt–accept–sample model,” *Physica A* **388**, 469–476 (2009).
- [52] G. Deffuant, “Comparing extremism propagation patterns in continuous opinion models,” *JASSS—the Journal of Artificial Societies and Social Simulation* **9**, (3)8 (2006).
- [53] R. Hegselmann and U. Krause, “Opinion dynamics and bounded confidence: Models, analysis and simulation,” *JASSS—the Journal of Artificial Societies and Social Simulation* **5**, (3)2 (2002).
- [54] G. Deffuant, D. Neau, F. Amblard, and G. Weisbuch, “Mixing beliefs among interacting agents,” *Advances in Complex Systems* **3**, 87 (2000).
- [55] F. W. S. Lima, “Kinetic continuous opinion dynamics model on two types of Archimedean lattices,” *Frontiers in Physics* **5**, 47 (2017).
- [56] K. Malarz, “Truth seekers in opinion dynamics models,” *International Journal of Modern Physics C* **17**, 1521–1524 (2006).
- [57] F. Baccelli, A. Chatterjee, and S. Vishwanath, “Pairwise stochastic bounded confidence opinion dynamics: Heavy tails and stability,” *IEEE Transactions on Automatic Control* **62**, 5678–5693 (2017).
- [58] W. Su, G. Chen, and Y. Hong, “Noise leads to quasi-consensus of Hegselmann–Krause opinion dynamics,” *Automatica* **85**, 448–454 (2017).
- [59] Y. Zhu, Q. A. Wang, W. Li, and X. Cai, “The formation of continuous opinion dynamics based on a gambling mechanism and its sensitivity analysis,” *Journal of Statistical Mechanics—Theory and Experiment* **2017**, 093401 (2017).
- [60] C. Anteneodo and N. Crokidakis, “Symmetry breaking by heating in a continuous opinion model,” *Physical Review E* **95**, 042308 (2017).
- [61] G. Chen, H. Cheng, C. Huang, W. Han, Q. Dai, H. Li, and J. Yang, “Deffuant model on a ring with repelling mechanism and circular opinions,” *Physical Review E* **95**, 042118 (2017).
- [62] Y. Zhang, Q. Liu, and S. Zhang, “Opinion formation with time-varying bounded confidence,” *PLoS ONE* **12**, e0172982 (2017).
- [63] Luca De Sanctis and Tobias Galla, “Effects of noise and confidence thresholds in nominal and metric axelrod dynamics of social influence,” *Physical Review E* **79**, 046108 (2009).
- [64] Jie Ren, Wen-Xu Wang, and Feng Qi, “Randomness enhances cooperation: A resonance-type phenomenon in evolutionary games,” *Physical Review E* **75**, 045101 (2007).
- [65] Alessio Emanuele Biondo, Alessandro Pluchino, and Andrea Rapisarda, “The beneficial role of random strategies in social and financial systems,” *Journal of Statistical Physics* **151**, 607–622 (2013).
- [66] Hirokazu Shirado and Nicholas A. Christakis, “Locally noisy autonomous agents improve global human coordination in network experiments,” *Nature* **545**, 370–374 (2017).
- [67] J. A. Holyst, K. Kacperski, and F. Schweitzer, “Social impact models of opinion dynamics,” in *Annual Reviews of Computational Physics IX*, edited by D. Stauffer (World Scientific, Singapore, 2011) pp. 253–273.
- [68] W. Gehrke, *Fortran 95 Language Guide* (Springer-Verlag, London, 1996).
- [69] P. Bańcerowski, “[www.zis.agh.edu.pl/app/MSc/Przemyslaw\\_Bancerowski/](http://www.zis.agh.edu.pl/app/MSc/Przemyslaw_Bancerowski/),” (2017).
- [70] J. Hoshen and R. Kopelman, “Percolation and cluster distribution. 1. Cluster multiple labeling technique and critical concentration algorithm,” *Physical Review B* **14**, 3438–3445 (1976).
- [71] M. Kotwica, P. Gronek, and K. Malarz, “Efficient space virtualisation for Hoshen–Kopelman algorithm,” *International Journal of Modern Physics C* **30**, 1950055 (2019).
- [72] K. Malarz, “Simple cubic random-site percolation thresholds for neighborhoods containing fourth-nearest neighbors,” *Physical Review E* **91**, 043301 (2015).
- [73] Ł. Kurzawski and K. Malarz, “Simple cubic random-site percolation thresholds for complex neighbourhoods,” *Reports on Mathematical Physics* **70**, 163–169 (2012).
- [74] M. Majewski and K. Malarz, “Square lattice site percolation thresholds for complex neighbourhoods,” *Acta Physica Polonica B* **38**, 2191–2199 (2007).
- [75] K. Malarz and S. Galam, “Square-lattice site percolation at increasing ranges of neighbor bonds,” *Physical Review E* **71**, 016125 (2005).
- [76] A. Carro, R. Toral, and M. San Miguel, “The noisy voter model on complex networks,” *Scientific Reports* **6**, 24775 (2016).
- [77] S. Galam, “Contrarian deterministic effects on opinion dynamics: ‘The hung elections scenario’,” *Physica A* **333**, 453–460 (2004).



### Appendix A: Example of small system evolution ( $L = 3, K = 3$ )

To better explain the model rules we calculate social impact on single actor for case of small lattice ( $L = 3$ ). We assume  $K = 3$  opinions available in the system marked as ‘red’ ( $\Xi_1$ ), ‘blue’ ( $\Xi_2$ ) and ‘green’ ( $\Xi_3$ ). We will calculate the impact exerting by nine actors on the actors labelled as ‘5’ and ‘9’ in Fig. 8. We assume the supportiveness  $s_i = i/10$  and persuasiveness  $p_i = 1 - i/10$ .

According to Eq. (2) to evaluate the opinion  $\xi_5(t+1)$  in the next time step we have to calculate  $K = 3$  impacts exerted on actor  $i = 5$  for three opinions available in the system.

As  $\xi_5(t) = \Xi_2$  (‘blue’) we use Eq. (2a) to calculate impact

$$I_{5,\text{blue}}(t) = 4\mathcal{J}_s \left( \frac{q(s_5)}{g(d_{5,5})} + \frac{q(s_6)}{g(d_{5,6})} + \frac{q(s_9)}{g(d_{5,9})} \right), \quad (\text{A1})$$

from all actors with ‘blue’ opinions (i.e. for  $i = 6, 9$ ), including actor  $i = 5$  himself/herself. The impacts from actors with ‘red’ and ‘green’ opinions are calculated basing on Eq. (2b):

$$I_{5,\text{red}}(t) = 4\mathcal{J}_p \left( \frac{q(p_1)}{g(d_{5,1})} + \frac{q(p_3)}{g(d_{5,3})} + \frac{q(p_4)}{g(d_{5,4})} + \frac{q(p_7)}{g(d_{5,7})} \right), \quad (\text{A2})$$

$$I_{5,\text{green}}(t) = 4\mathcal{J}_p \left( \frac{q(p_2)}{g(d_{5,2})} + \frac{q(p_8)}{g(d_{5,8})} \right), \quad (\text{A3})$$



FIG. 8: (Colour online) Example of small lattice with nine actors and three opinions. The numbers are actors labels  $i$ . The colours correspond to various actors opinions (‘red’— $\Xi_1$ , ‘blue’— $\Xi_2$  and ‘green’— $\Xi_3$ ).

We assume identity function for scaling functions  $\mathcal{J}_S(x) \equiv x$ ,  $\mathcal{J}_P(x) \equiv x$ ,  $q(x) \equiv x$  and the distance scaling function  $g(x) = 1 + x^\alpha$ , with  $\alpha = 2$ . These assumptions yield

$$I_{5,\text{blue}}(t) = 4 \left( \frac{s_5}{1 + d_{5,5}^2} + \frac{s_6}{1 + d_{5,6}^2} + \frac{s_9}{1 + d_{5,9}^2} \right) = 4 \left( \frac{0.5}{1 + 0^2} + \frac{0.6}{1 + 1^2} + \frac{0.9}{1 + \sqrt{2}^2} \right) = 4.4, \quad (\text{A4})$$

$$\begin{aligned} I_{5,\text{red}}(t) &= 4 \left( \frac{p_1}{1 + d_{5,1}^2} + \frac{p_3}{1 + d_{5,3}^2} + \frac{p_4}{1 + d_{5,4}^2} + \frac{p_7}{1 + d_{5,7}^2} \right) \\ &= 4 \left( \frac{0.9}{1 + \sqrt{2}^2} + \frac{0.7}{1 + \sqrt{2}^2} + \frac{0.6}{1 + 1^2} + \frac{0.3}{1 + \sqrt{2}^2} \right) = 7.(3), \quad (\text{A5}) \end{aligned}$$

$$I_{5,\text{green}}(t) = 4 \left( \frac{p_2}{1 + d_{5,2}^2} + \frac{p_8}{1 + d_{5,8}^2} \right) = 4 \left( \frac{0.8}{1 + 1^2} + \frac{0.2}{1 + 1^2} \right) = 2. \quad (\text{A6})$$

For  $T = 0$  the largest impact on actor  $i = 5$  is exerted by ‘red’ actors and thus—according to Eq. (1)—actor  $i = 5$  in the next time step **will change** his/her opinion from ‘blue’ ( $\xi_5(t) = \Xi_2$ ) to ‘red’ ( $\xi_5(t+1) = \Xi_1$ ).

For  $T > 0$  we calculate probabilities  $P_{5,\text{blue}}$ ,  $P_{5,\text{red}}$  and  $P_{5,\text{green}}$  of choosing opinion by actor  $i = 5$  (see Eqs. (4a)–(4b)). For example, for  $T = 1$  these probabilities are

$$\begin{aligned} P_{5,\text{blue}} &= \frac{\exp(I_{5,\text{blue}}/1)}{P_1}, \\ P_{5,\text{red}} &= \frac{\exp(I_{5,\text{red}}/1)}{P_1}, \\ P_{5,\text{green}} &= \frac{\exp(I_{5,\text{green}}/1)}{P_1}, \end{aligned} \quad (\text{A7})$$

while for  $T = 10$  we have

$$\begin{aligned} P_{5,\text{blue}} &= \frac{\exp(I_{5,\text{blue}}/10)}{P_{10}}, \\ P_{5,\text{red}} &= \frac{\exp(I_{5,\text{red}}/10)}{P_{10}}, \\ P_{5,\text{green}} &= \frac{\exp(I_{5,\text{green}}/10)}{P_{10}}, \end{aligned} \quad (\text{A8})$$

where normalisation constants are

$$P_1 = \exp(I_{5,\text{blue}}/1) + \exp(I_{5,\text{red}}/1) + \exp(I_{5,\text{green}}/1)$$

and

$$P_{10} = \exp(I_{5,\text{blue}}/10) + \exp(I_{5,\text{red}}/10) + \exp(I_{5,\text{green}}/10).$$

The calculated probabilities for  $T = 1$  are

$$\begin{aligned} P_{5,\text{blue}} &= \frac{\exp(4.4/1)}{e^{4.4} + e^{7.(3)} + e^2} \approx 0.050, \\ P_{5,\text{red}} &= \frac{\exp(7.(3)/1)}{e^{4.4} + e^{7.(3)} + e^2} \approx 0.945, \\ P_{5,\text{green}} &= \frac{\exp(2/1)}{e^{4.4} + e^{7.(3)} + e^2} \approx 0.005, \end{aligned} \quad (\text{A9})$$

while for  $T = 10$  we have

$$\begin{aligned} P_{5,\text{blue}} &= \frac{\exp(4.4/10)}{e^{0.44} + e^{0.7(3)} + e^{0.2}} \approx 0.320, \\ P_{5,\text{red}} &= \frac{\exp(7.(3)/10)}{e^{0.44} + e^{0.7(3)} + e^{0.2}} \approx 0.429, \\ P_{5,\text{green}} &= \frac{\exp(2/10)}{e^{0.44} + e^{0.7(3)} + e^{0.2}} \approx 0.251. \end{aligned} \quad (\text{A10})$$

For non-deterministic version of algorithm (i.e. for  $T > 0$ ) still the most probably state  $\xi_5(t+1)$  is  $\Xi_1$  ('red'). But probability of such evolution for actor  $i = 5$  decreases from 100% for  $T = 0$  to 94.5% for  $T = 1$  and to 42.9% for  $T = 10$  to become  $33.3\% = 1/K$  for  $T \rightarrow \infty$ .

Let us repeat these calculation for actor  $i = 9$ :

$$I_{9,\text{blue}}(t) = 4\mathcal{J}_s \left( \frac{q(s_5)}{g(d_{9,5})} + \frac{q(s_6)}{g(d_{9,6})} + \frac{q(s_9)}{g(d_{9,9})} \right), \quad (\text{A11})$$

$$I_{9,\text{red}}(t) = 4\mathcal{J}_p \left( \frac{q(p_1)}{g(d_{9,1})} + \frac{q(p_3)}{g(d_{9,3})} + \frac{q(p_4)}{g(d_{9,4})} + \frac{q(p_7)}{g(d_{9,7})} \right), \quad (\text{A12})$$

$$I_{9,\text{green}}(t) = 4\mathcal{J}_p \left( \frac{q(p_2)}{g(d_{9,2})} + \frac{q(p_8)}{g(d_{9,8})} \right), \quad (\text{A13})$$

$$I_{9,\text{blue}}(t) = 4 \left( \frac{s_5}{1 + d_{9,5}^2} + \frac{s_6}{1 + d_{9,6}^2} + \frac{s_9}{1 + d_{9,9}^2} \right) = 4 \left( \frac{0.5}{1 + \sqrt{2}^2} + \frac{0.6}{1 + 1^2} + \frac{0.9}{1 + 0^2} \right) = 5.4(6), \quad (\text{A14})$$

$$\begin{aligned} I_{9,\text{red}}(t) &= 4 \left( \frac{p_1}{1 + d_{9,1}^2} + \frac{p_3}{1 + d_{9,3}^2} + \frac{p_4}{1 + d_{9,4}^2} + \frac{p_7}{1 + d_{9,7}^2} \right) \\ &= 4 \left( \frac{0.9}{1 + (2\sqrt{2})^2} + \frac{0.7}{1 + 2^2} + \frac{0.6}{1 + \sqrt{5}^2} + \frac{0.3}{1 + 2^2} \right) = 1.6, \end{aligned} \quad (\text{A15})$$

$$I_{9,\text{green}}(t) = 4 \left( \frac{p_2}{1 + d_{9,2}^2} + \frac{p_8}{1 + d_{9,8}^2} \right) = 4 \left( \frac{0.8}{1 + \sqrt{5}^2} + \frac{0.2}{1 + 1^2} \right) = 0.9(3). \quad (\text{A16})$$

For  $T = 0$  the largest impact on actor  $i = 9$  is exerted by ‘blue’ actors and thus—according to Eq. (1)—actor  $i = 9$  in the next time step **will sustain** his/her ‘blue’ opinion ( $\xi_9(t+1) = \xi_9(t) = \Xi_2$ ). Two factors influence the difference in actors  $i = 5$  and  $i = 9$  opinion in time  $(t + 1)$ . Namely, the difference in supportiveness of these two actors and their distance to ‘red’ actors: actor  $i = 5$  has moderate supportiveness ( $s_5 = 0.5$ ) and his/her distance to ‘red’ actors is no longer than  $\sqrt{2}$ . In contrast, actor  $i = 9$  has very high supportiveness ( $s_9 = 0.9$ ) and distance to ‘red’ actors no shorter than 2. Please note however, that ultimate fate of the system is the state with the unanimity of opinions. As we have shown above, in the next time step at least the actor in the middle of the system ( $i = 5$ ) will convert his/her opinion to the ‘red’ one. The same presumably will occur for actor  $i = 2$  who has low supportiveness ( $s_2 = 0.2$ ) and who has only a single supporter. Thus in time  $(t + 3)$  all actors will convert to the supporters of the ‘red’ opinion.

For  $T > 0$  we calculate probabilities  $P_{9,\text{blue}}$ ,  $P_{9,\text{red}}$  and  $P_{9,\text{green}}$  of choosing opinion by actor  $i = 9$  (see Eqs. (4a)–(4b)). For example, for  $T = 1$  these probabilities are

$$\begin{aligned} P_{9,\text{blue}} &= \frac{\exp(I_{9,\text{blue}}/1)}{P_1}, \\ P_{9,\text{red}} &= \frac{\exp(I_{9,\text{red}}/1)}{P_1}, \\ P_{9,\text{green}} &= \frac{\exp(I_{9,\text{green}}/1)}{P_1}, \end{aligned} \quad (\text{A17})$$

while for  $T = 10$  we have

$$\begin{aligned} P_{9,\text{blue}} &= \frac{\exp(I_{9,\text{blue}}/10)}{P_{10}}, \\ P_{9,\text{red}} &= \frac{\exp(I_{9,\text{red}}/10)}{P_{10}}, \\ P_{9,\text{green}} &= \frac{\exp(I_{9,\text{green}}/10)}{P_{10}}, \end{aligned} \quad (\text{A18})$$

where normalisation constants are

$$P_1 = \exp(I_{9,\text{blue}}/1) + \exp(I_{9,\text{red}}/1) + \exp(I_{9,\text{green}}/1)$$

and

$$P_{10} = \exp(I_{9,\text{blue}}/10) + \exp(I_{9,\text{red}}/10) + \exp(I_{9,\text{green}}/10).$$

The calculated probabilities for  $T = 1$  are

$$\begin{aligned} P_{9,\text{blue}} &= \frac{\exp(5.4(6)/1)}{e^{5.4(6)} + e^{1.6} + e^{0.9(3)}} \approx 0.969, \\ P_{9,\text{red}} &= \frac{\exp(1.6/1)}{e^{5.4(6)} + e^{1.6} + e^{0.9(3)}} \approx 0.020, \\ P_{9,\text{green}} &= \frac{\exp(0.9(3)/1)}{e^{5.4(6)} + e^{1.6} + e^{0.9(3)}} \approx 0.011, \end{aligned} \quad (\text{A19})$$

while for  $T = 10$  we have

$$\begin{aligned} P_{9,\text{blue}} &= \frac{\exp(5.4(6)/10)}{e^{0.54(6)} + e^{0.16} + e^{0.09(3)}} \approx 0.432, \\ P_{9,\text{red}} &= \frac{\exp(1.6/10)}{e^{0.54(6)} + e^{0.16} + e^{0.09(3)}} \approx 0.293, \\ P_{9,\text{green}} &= \frac{\exp(0.9(3)/10)}{e^{0.54(6)} + e^{0.16} + e^{0.09(3)}} \approx 0.275. \end{aligned} \quad (\text{A20})$$

Similarly to the actor  $i = 5$ , the increase of the social temperature reduces chance of keeping initial opinion for actor  $i = 9$ . For  $T = 10$  these probabilities do not differ from  $1/K$  for more than 0.1.

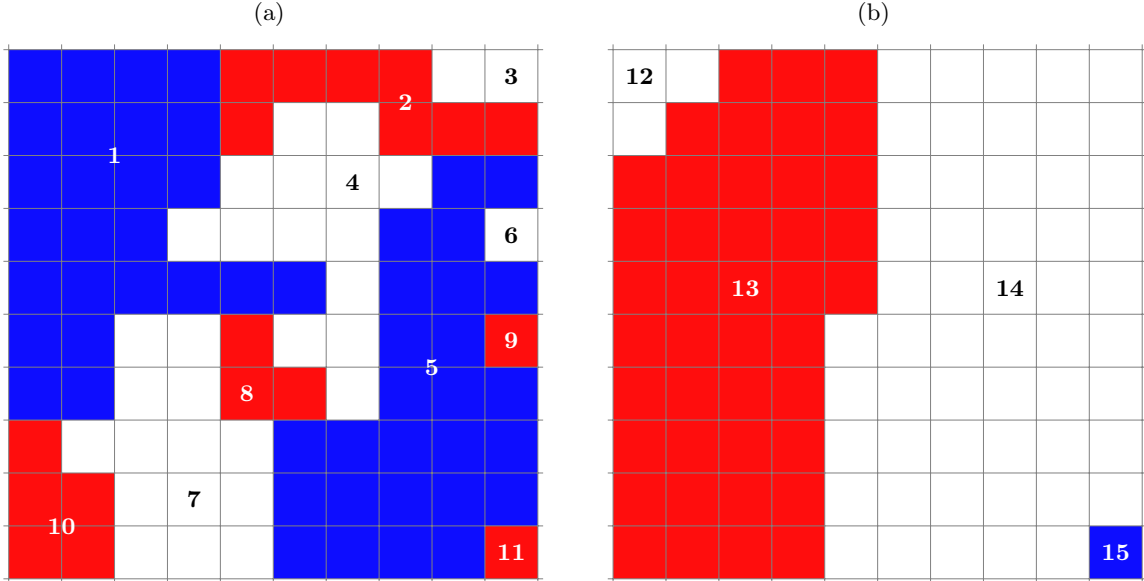


TABLE I: Histogram of cluster sizes  $\mathcal{S}$  for lattices presented in Fig. 9.

labels $i$ :	6, 9, 11, 15	3	8, 12	10	2	4, 7	1, 5	13	14
$\mathcal{S}$ :	1	2	3	5	8	14	25	42	54
$n(\mathcal{S})$ :	4	1	2	1	1	2	2	1	1

### Appendix B: Small example of clustering ( $L = 10, K = 3$ )

Two sites are in the same cluster if they are adjacent (in von Neumann neighbourhood, Fig. 5) to each other and simultaneously actors at these sites share the same opinion. The Hoshen–Kopelman algorithm allows for sites labelling in such way that sites in the same cluster have the same labels and sites in different cluster have different labels. Examples of sites labelling for  $L = 10$  and  $K = 3$  are presented in Figs. 9a and 9b, where  $n_c = 11$  and  $n_c = 4$  clusters have been identified, respectively. The average number of cluster for these two lattice realization is  $\langle n_c \rangle = (11 + 4)/2 = 7.5$ . The number of sites in each cluster defines its size  $\mathcal{S}$ . For these two lattice realizations the largest culsters are labelled as 1 and 5 (Fig. 9a) and as 14 (Fig. 9b) and their sizes are  $\mathcal{S}_{\max} = 25$  and  $\mathcal{S}_{\max} = 54$ , respectively. Thus average largest cluster size is  $\langle \mathcal{S}_{\max} \rangle = (25 + 54)/2 = 39.5$ . In given example histogram  $H(\mathcal{S})$  of clusters sizes is presented in Table I. Basing on Table I we evaluate number of small clusters (with  $\mathcal{S} \leq 5$ ) as  $4+1+2+1=8$ . As this sum comes from merging results of two lattice realization the average number of small clusters is  $\langle n_s \rangle = 8/2 = 4$ .

FIG. 9: Example of sites labelling for  $K = 3$  and  $L = 10$  and two lattice realizations.

### Appendix C: Source codes

In Listings 1 and 2 the Fortran 95 codes allowing for reproductions of data for Figs. 3, 4, 6, 7 (for both, noiseless and non-deterministic version of simulations) are presented.

The module `settings` provides model parameters including lattice size  $L$  (`Xmax` and `Ymax`), number of opinions  $K$  (`Kmax`), number of time steps  $t_{\max}$  (`Tmax`) and number of lattice realizations (`Run`).

In module `utils` the scaling functions  $g(x)$  and  $q(x)$  as well as the Euclidean distance  $d(x, y)$  are defined. Also the `reclassify` function for Hoshen–Kopelman algorithm is defined there.

The main program starts in line 52. The actors supportiveness ( $s_i$ ) and persuasiveness ( $p_i$ ) are initialised randomly in lines 85–90, while initial actors opinions ( $\xi_i$ ) are given in lines 93–98. Loop 88 provides time evolution of the system. Loop 77 realises Hoshen–Kopelman algorithm of sites (actors) labelling for  $t = 0$ . In loop 99 the system

characteristics after the system time evolution is completed are calculated. Loop 777 realises averaging procedure over independent runnings for various initial conditions.

### 1. $T = 0$

An input data ( $\alpha$  parameter) is read in line 71. In lines 272–275 histograms  $H(\mathcal{S})$  of clusters sizes  $\mathcal{S}$  are printed. In line 278 values of  $\langle n_c \rangle$ ,  $\langle S \rangle$  (not presented in this paper) and  $\langle S_{\max} \rangle$  are printed.

Listing 1: Fortran95 code implementing Eq. (1) i.e. for  $T = 0$

```

1  !!! Latane-Nowak-Szamrej model + Hoshen-Kopelman algorithm
2  !!! K. Malarz
3  !!! created: Tue, 21 May 2019, 13:06:13 CEST
4  !!! revised: Sun, 05 Apr 2020, 14:43:19 CEST
5
6  !!! =====
7  module settings
8  !!! =====
9  implicit none
10
11 integer, parameter :: Xmax=41,Ymax=41,Tmax=1000,Kmax=2,L2=(Xmax+1)*(Ymax+1),Run=100
12 real*8, parameter :: T=0.d0
13 real*8 :: alpha
14 end module settings
15
16 !!! =====
17 module utils
18 !!! =====
19 use settings
20 implicit none
21 contains
22
23 real*8 function g(x)
24     real*8 :: x
25     g=1.0d0+x**alpha
26 end function
27
28 real*8 function q(x)
29     real*8 :: x
30     q=x
31 end function
32
33 real*8 function d(x1,y1,x2,y2)
34     integer :: x1,y1,x2,y2
35     d=dsqrt((1.d0*x1-1.d0*x2)**2 + (1.d0*y1-1.d0*y2)**2)
36 end function
37
38 integer function reclassify(ix)
39 integer :: ix
40 integer, dimension (0:Xmax,0:Ymax) :: label
41 integer, dimension (L2) :: iclass
42 common/block/ label, iclass
43
44 reclassify=iclass(ix)
45 90 if(iclass(reclassify).eq.reclassify) return
46 reclassify=iclass(reclassify)
47 goto 90
48 end function
49
50 end module utils
51
52 !!! #####
53 program Latane_Hoshen_Kopelman
54 !!! #####
55 use settings
56 use utils
57 implicit none
58 integer :: x,y,it , xx,yy,k,kk,strongest_k , irun , maxlabel , Smax , largestS

```

```

59 real :: r
60 real*8 :: sump, strongest_I , avenc , aveS , aveSmax
61
62 integer , dimension (0:Xmax,0:Ymax) :: label
63 integer , dimension (L2) :: iclass
64 integer , dimension (0:Xmax,0:Ymax) :: xi
65 integer , dimension (0:Xmax*Ymax) :: isize , histograminrun , histogram
66 integer , dimension (0:Xmax*Ymax,Kmax) :: histogramK
67 real*8 , dimension (Xmax,Ymax) :: p , s
68 real*8 , dimension (Xmax,Ymax,Kmax) :: I , prob
69 common/block/ label , iclass
70
71 read *,alpha
72 print '(A3,7A11) ', '###', 'Xmax', 'Ymax', 'K', 'alpha', 'T', 'tmax', 'run'
73 print '(A3,3I11,2F11.3,2I11) ', '###', Xmax, Ymax, Kmax, alpha , T, Tmax, Run
74
75 histogram=0
76 aveSmax=0.d0
77 aveS=0.d0
78 avenc=0.d0
79
80 do 777 irun=1,Run
81 histograminrun=0
82 ! print *,'#####'
83 ! print *,'# irun=',irun
84
85 do x=1,Xmax !! initial state
86 do y=1,Ymax
87 s(x,y)=rand()
88 p(x,y)=rand()
89 enddo
90 enddo
91
92 it=0
93 xi=0
94 do x=1,Xmax
95 do y=1,Ymax
96 xi(x,y)=1+Kmax*rand()
97 enddo
98 enddo
99
100 histogramK=0
101
102 do 77 k=1,Kmax
103 isize=0
104
105 label=L2
106 do kk=1,L2
107 iclass(kk)=kk
108 enddo
109 maxlabel=0
110
111 do x=1,Xmax
112 do y=1,Ymax
113 if(xi(x,y).eq.k) then !! labeling clusters
114 if(xi(x-1,y).eq.k .or. xi(x,y-1).eq.k) then
115 !! reclassifying neighbouring sites
116 if(xi(x-1,y).eq.k) label(x-1,y)=reclassify(label(x-1,y))
117 if(xi(x,y-1).eq.k) label(x,y-1)=reclassify(label(x,y-1))
118 label(x,y)=min(label(x-1,y),label(x,y-1))
119 iclass(label(x-1,y))=label(x,y)
120 iclass(label(x,y-1))=label(x,y)
121 else
122 maxlabel=maxlabel+1
123 label(x,y)=maxlabel
124 endif
125 enddo
126 enddo
127 enddo
128 ! reclassifying all occupied sites

```

```

129 do x=1,Xmax
130 do y=1,Ymax
131   if ((xi(x,y).eq.k) .and. (label(x,y).gt.iclass(label(x,y)))) label(x,y)=reclassify(label(x,y))
132 enddo
133 enddo
134
135 do x=1,Xmax
136 do y=1,Ymax
137   if (xi(x,y).eq.k) isize(label(x,y))=isize(label(x,y))+1
138 enddo
139 enddo
140
141 do kk=1,Xmax*Ymax
142   histogramK(isize(kk),k)=histogramK(isize(kk),k)+1
143 enddo
144
145 77 enddo
146
147 do 88 it=1,Tmax !!! time evolution
148   I=0.0d0
149   do x=1,Xmax
150   do y=1,Ymax
151   do xx=1,Xmax
152   do yy=1,Ymax
153     if (xi(x,y).eq.xi(xx,yy)) then
154       I(x,y,xi(xx,yy))=I(x,y,xi(xx,yy))+q(s(xx,yy))/g(d(x,y,xx,yy))
155     else
156       I(x,y,xi(xx,yy))=I(x,y,xi(xx,yy))+q(p(xx,yy))/g(d(x,y,xx,yy))
157     endif
158   enddo
159   enddo
160 enddo
161 enddo
162
163 do x=1,Xmax
164 do y=1,Ymax
165 do k=1,Kmax
166   I(x,y,k)=4.0d0*I(x,y,k)
167 enddo
168 enddo
169 enddo
170
171 do x=1,Xmax
172 do y=1,Ymax
173   strongest_I=I(x,y,1)
174   strongest_k=1
175   do k=2,Kmax
176     if (I(x,y,k).gt.strongest_I) then
177       strongest_I=I(x,y,k)
178       strongest_k=k
179     endif
180   enddo
181   xi(x,y)=strongest_k
182 enddo
183 enddo
184 88 enddo !!! time evolution
185
186 ! print *,'# it=',it,'xi:'
187 ! do x=1,Xmax
188 ! print '(4115)',(xi(x,y),y=1,Ymax)
189 ! enddo
190 histogramK=0
191 Smax=0
192
193 do 99 k=1,Kmax
194   isize=0
195
196 ! print *,'# k=',k
197 label=L2
198 do kk=1,L2

```

```

199   iclass(kk)=kk
200   enddo
201   maxlabel=0
202
203   do x=1,Xmax
204   do y=1,Ymax
205     if(xi(x,y).eq.k) then ! labeling clusters
206       if(xi(x-1,y).eq.k .or. xi(x,y-1).eq.k) then
207         ! reclassifying neighbouring sites
208         if(xi(x-1,y).eq.k) label(x-1,y)=reclassify(label(x-1,y))
209         if(xi(x,y-1).eq.k) label(x,y-1)=reclassify(label(x,y-1))
210         label(x,y)=min(label(x-1,y),label(x,y-1))
211         iclass(label(x-1,y))=label(x,y)
212         iclass(label(x,y-1))=label(x,y)
213       else
214         maxlabel=maxlabel+1
215         label(x,y)=maxlabel
216       endif
217     endif
218   enddo
219   enddo
220   ! reclassifying all occupied sites
221   do x=1,Xmax
222   do y=1,Ymax
223     if((xi(x,y).eq.k) .and. (label(x,y).gt.iclass(label(x,y)))) label(x,y)=reclassify(label(x,y))
224   enddo
225   enddo
226
227   ! do x=1,Xmax
228   ! print '(4115)',(label(x,y),y=1,Ymax)
229   ! enddo
230
231   do x=1,Xmax
232   do y=1,Ymax
233     if(xi(x,y).eq.k) isize(label(x,y))=isize(label(x,y))+1
234   enddo
235   enddo
236
237   do kk=1,Xmax*Ymax
238     histogramK(isize(kk),k)=histogramK(isize(kk),k)+1
239   enddo
240
241   ! print *, "# histogram, irun=", irun, " k=", k
242   do kk=1,Xmax*Ymax
243   ! if(histogramK(kk,k).gt.0) print *,kk,histogramK(kk,k)
244     histograminrun(kk)=histograminrun(kk)+histogramK(kk,k)
245   enddo
246
247   do kk=Xmax*Ymax,1,-1
248     if(histogramK(kk,k).gt.0) then
249       largestS=kk
250       goto 33
251     endif
252   enddo
253   33 Smax=max(Smax, largestS)
254   ! print *, "# largest S=", largestS
255   ! print *, "# Smax=", Smax
256
257   99 enddo
258
259   ! do k=1,Xmax*Ymax
260   ! if(histograminrun(k).gt.0) print *,k,histograminrun(k)
261   ! enddo
262   ! print *, "# nc=", sum(histograminrun)
263   avenc=avenc+1.d0*sum(histograminrun)
264   aveSmax=aveSmax+1.d0*Smax
265   do k=1,Xmax*Ymax
266     aveS=aveS+(1.d0*k*histograminrun(k))/(1.d0*sum(histograminrun))
267     histogram(k)=histogram(k)+histograminrun(k)
268   enddo

```



```

269 777 enddo
270
271 print *, "#_total_histogram:"
272 do k=1,Xmax*Ymax
273   if (histogram(k).gt.0) print *,k,histogram(k)
274 enddo
275
276 print '(A2,A3,5A9)',"#","K","T","alpha","<nc>","<S>","<Smax>"
277 print '(A2,I3,5F9.3)',"#",Kmax,T,alpha,avenc/(1.d0*Run),aveS/(1.d0*Run),aveSmax/(1.d0*Run)
278
279 end program Latane_Hoshen_Kopelman
280

```

## 2. $T > 0$

An input data ( $\alpha$  and  $T$  parameters) are read in line 71. In lines 284–287 histograms  $H(S)$  of clusters size  $S$  are printed. In line 290 values of  $\langle n_c \rangle$ ,  $\langle S \rangle$  (not presented in this paper),  $\langle S_{\max} \rangle$  are printed.

Listing 2: Fortran95 code implementing Eq. (4) i.e. for  $T > 0$

```

1  !!! Latane-Nowak-Szamrej model + Hoshen-Kopelman algorithm
2  !!! K. Malarz
3  !!! created: Tue, 21 May 2019, 13:06:13 CEST
4  !!! revised: Sun, 05 Apr 2020, 14:43:19 CEST
5
6  !!! =====
7  module settings
8  !!! =====
9  implicit none
10
11 integer, parameter :: Xmax=41,Ymax=41,Tmax=1000,Kmax=2,L2=(Xmax+1)*(Ymax+1),Run=100
12 real*8 :: T
13 real*8 :: alpha
14 end module settings
15
16 !!! =====
17 module utils
18 !!! =====
19 use settings
20 implicit none
21 contains
22
23 real*8 function g(x)
24   real*8 :: x
25   g=1.0d0+x**alpha
26 end function
27
28 real*8 function q(x)
29   real*8 :: x
30   q=x
31 end function
32
33 real*8 function d(x1,y1,x2,y2)
34   integer :: x1,y1,x2,y2
35   d=dsqrt((1.d0*x1-1.d0*x2)**2 + (1.d0*y1-1.d0*y2)**2)
36 end function
37
38 integer function reclassify(ix)
39 integer :: ix
40 integer, dimension (0:Xmax,0:Ymax) :: label
41 integer, dimension (L2) :: iclass
42 common/block/ label, iclass
43
44 reclassify=iclass(ix)
45 90 if(iclass(reclassify).eq.reclassify) return
46 reclassify=iclass(reclassify)
47 goto 90
48 end function

```

```

49 end module utils
50
51
52 !!! #####
53 program Latane_Hoshen_Kopelman
54 !!! #####
55 use settings
56 use utils
57 implicit none
58 integer :: x,y,it , xx,yy,k,kk,strongest_k , irun , maxlabel ,Smax ,largestS
59 real :: r
60 real*8 :: sump,avenc,aveS,aveSmax
61
62 integer , dimension (0:Xmax,0:Ymax) :: label
63 integer , dimension (L2) :: iclass
64 integer , dimension (0:Xmax,0:Ymax) :: xi
65 integer , dimension (0:Xmax*Ymax) :: isize , histograminrun , histogram
66 integer , dimension (0:Xmax*Ymax,Kmax) :: histogramK
67 real*8 , dimension (Xmax,Ymax) :: p, s
68 real*8 , dimension (Xmax,Ymax,Kmax) :: I, prob
69 common/block/ label, iclass
70
71 read *,T,alpha
72 print '(A3,7A11)', '###', 'Xmax', 'Ymax', 'K', 'alpha', 'T', 'tmax', 'run'
73 print '(A3,3I11,2F11.3,2I11)', '###', Xmax, Ymax, Kmax, alpha ,T, Tmax, Run
74
75 histogram=0
76 aveSmax=0.d0
77 aveS=0.d0
78 avenc=0.d0
79
80 do 777 irun=1,Run
81 histograminrun=0
82 ! print *,'#####'
83 ! print *,'# irun=',irun
84
85 do x=1,Xmax !! initial state
86 do y=1,Ymax
87 s(x,y)=rand()
88 p(x,y)=rand()
89 enddo
90 enddo
91
92 it=0
93 xi=0
94 do x=1,Xmax
95 do y=1,Ymax
96 xi(x,y)=1+Kmax*rand()
97 enddo
98 enddo
99
100 histogramK=0
101
102 do 77 k=1,Kmax
103 isize=0
104
105 label=L2
106 do kk=1,L2
107 iclass(kk)=kk
108 enddo
109 maxlabel=0
110
111 do x=1,Xmax
112 do y=1,Ymax
113 if(xi(x,y).eq.k) then !! labeling clusters
114 if(xi(x-1,y).eq.k .or. xi(x,y-1).eq.k) then
115 !! reclassifying neighbouring sites
116 if(xi(x-1,y).eq.k) label(x-1,y)=reclassify(label(x-1,y))
117 if(xi(x,y-1).eq.k) label(x,y-1)=reclassify(label(x,y-1))
118 label(x,y)=min(label(x-1,y),label(x,y-1))

```

```

119         iclass (label(x-1,y))=label(x,y)
120         iclass (label(x,y-1))=label(x,y)
121     else
122         maxlabel=maxlabel+1
123         label(x,y)=maxlabel
124     endif
125 endif
126 enddo
127 enddo
128 ! reclassifying all occupied sites
129 do x=1,Xmax
130 do y=1,Ymax
131     if ((xi(x,y).eq.k) .and. (label(x,y).gt.iclass(label(x,y)))) label(x,y)=reclassify(label(x,y))
132 enddo
133 enddo
134
135 do x=1,Xmax
136 do y=1,Ymax
137     if (xi(x,y).eq.k) isize(label(x,y))=isize(label(x,y))+1
138 enddo
139 enddo
140
141 do kk=1,Xmax*Ymax
142     histogramK(isize(kk),k)=histogramK(isize(kk),k)+1
143 enddo
144
145 77 enddo
146
147 do 88 it=1,Tmax !!! time evolution
148     I=0.0d0
149     do x=1,Xmax
150     do y=1,Ymax
151         do xx=1,Xmax
152         do yy=1,Ymax
153             if (xi(x,y).eq.xi(xx,yy)) then
154                 I(x,y,xi(xx,yy))=I(x,y,xi(xx,yy))+q(s(xx,yy))/g(d(x,y,xx,yy))
155             else
156                 I(x,y,xi(xx,yy))=I(x,y,xi(xx,yy))+q(p(xx,yy))/g(d(x,y,xx,yy))
157             endif
158         enddo
159     enddo
160     enddo
161     enddo
162
163     do x=1,Xmax
164     do y=1,Ymax
165     do k=1,Kmax
166         I(x,y,k)=4.0d0*I(x,y,k)
167     enddo
168     enddo
169     enddo
170
171     do x=1,Xmax
172     do y=1,Ymax
173         sump=0.0d0
174         do k=1,Kmax
175             prob(x,y,k)=dexp(I(x,y,k)/T)
176             sump=sump+prob(x,y,k)
177         enddo
178         do k=1,Kmax
179             prob(x,y,k)=prob(x,y,k)/sump
180         enddo
181     enddo
182     enddo
183
184     do x=1,Xmax
185     do y=1,Ymax
186         r=rand()
187         sump=0.0d0
188         do k=1,Kmax

```

```

189     sump=sump+prob(x,y,k)
190     if(r.lt.sump) goto 666
191     enddo
192 666     xi(x,y)=k
193     enddo
194     enddo
195
196 88 enddo !!! time evolution
197
198 ! print *,'# it=',it,'xi:'
199 ! do x=1,Xmax
200 ! print '(4115)',(xi(x,y),y=1,Ymax)
201 ! enddo
202 histogramK=0
203 Smax=0
204
205 do 99 k=1,Kmax
206     isize=0
207
208 ! print *,"# k=",k
209     label=L2
210     do kk=1,L2
211         iclass(kk)=kk
212     enddo
213     maxlabel=0
214
215     do x=1,Xmax
216     do y=1,Ymax
217         if(xi(x,y).eq.k) then ! labeling clusters
218             if(xi(x-1,y).eq.k .or. xi(x,y-1).eq.k) then
219                 ! reclassifying neighbouring sites
220                 if(xi(x-1,y).eq.k) label(x-1,y)=reclassify(label(x-1,y))
221                 if(xi(x,y-1).eq.k) label(x,y-1)=reclassify(label(x,y-1))
222                 label(x,y)=min(label(x-1,y),label(x,y-1))
223                 iclass(label(x-1,y))=label(x,y)
224                 iclass(label(x,y-1))=label(x,y)
225             else
226                 maxlabel=maxlabel+1
227                 label(x,y)=maxlabel
228             endif
229         endif
230     enddo
231     enddo
232     ! reclassifying all occupied sites
233     do x=1,Xmax
234     do y=1,Ymax
235         if((xi(x,y).eq.k) .and. (label(x,y).gt.iclass(label(x,y)))) label(x,y)=reclassify(label(x,y))
236     enddo
237     enddo
238
239 ! do x=1,Xmax
240 ! print '(4115)',(label(x,y),y=1,Ymax)
241 ! enddo
242
243 do x=1,Xmax
244 do y=1,Ymax
245     if(xi(x,y).eq.k) isize(label(x,y))=isize(label(x,y))+1
246 enddo
247 enddo
248
249 do kk=1,Xmax*Ymax
250     histogramK(isize(kk),k)=histogramK(isize(kk),k)+1
251 enddo
252
253 ! print *,"# histogram, irun=",irun," k=",k
254 do kk=1,Xmax*Ymax
255 ! if(histogramK(kk,k).gt.0) print *,kk,histogramK(kk,k)
256     histograminrun(kk)=histograminrun(kk)+histogramK(kk,k)
257 enddo
258

```

```

259   do kk=Xmax*Ymax,1,-1
260     if (histogramK(kk,k).gt.0) then
261       largestS=kk
262       goto 33
263     endif
264   enddo
265 33 Smax=max(Smax,largestS)
266 !   print *,"# largest S=",largestS
267 !   print *,"# Smax=",Smax
268
269 99 enddo
270
271 !   do k=1,Xmax*Ymax
272 !     if (histograminrun(k).gt.0) print *,k,histograminrun(k)
273 !   enddo
274 !   print *,"# nc=",sum(histograminrun)
275   avenc=avenc+1.d0*sum(histograminrun)
276   aveSmax=aveSmax+1.d0*Smax
277   do k=1,Xmax*Ymax
278     aveS=aveS+(1.d0*k*histograminrun(k))/(1.d0*sum(histograminrun))
279     histogram(k)=histogram(k)+histograminrun(k)
280   enddo
281
282 777 enddo
283
284   print *,"#_total_histogram:"
285   do k=1,Xmax*Ymax
286     if (histogram(k).gt.0) print *,k,histogram(k)
287   enddo
288
289   print '(A2,A3,5A9)',"#","K","T","alpha", "<nc>", "<S>", "<Smax>"
290   print '(A2,I3,5F9.3)',"#",Kmax,T,alpha,avenc/(1.d0*Run),aveS/(1.d0*Run),aveSmax/(1.d0*Run)
291
292 end program Latane_Hoshen_Kopelman

```